

# The probe technique far-from-equilibrium: Magnetic field symmetries of nonlinear transport

Salil Bedkihal<sup>1</sup>, Malay Bandyopadhyay<sup>2</sup>, Dvira Segal<sup>1</sup>

<sup>1</sup> *Chemical Physics Theory Group, Department of Chemistry, University of Toronto,  
80 Saint George St. Toronto, Ontario, Canada M5S 3H6 and*

<sup>2</sup> *School of Basic Sciences, Indian Institute of Technology Bhubaneswar, 751007, India*  
(Dated: August 16, 2018)

The probe technique is a simple mean to incorporate elastic and inelastic processes into quantum dynamics. Using numerical simulations, we demonstrate that this tool can be employed beyond the analytically tractable linear response regime, providing a stable solution for the probe parameters: temperature and chemical potential. Adopting four probes: dephasing, voltage, temperature, and voltage-temperature, mimicking different elastic and inelastic effects, we focus on magnetic field and gate voltage symmetries of charge current and heat current in Aharonov-Bohm interferometers, potentially far-from-equilibrium. Considering electron current, we prove analytically that in the linear response regime inelastic scattering processes do not break the Onsager symmetry. Beyond linear response, even (odd) conductance terms obey an odd (even) symmetry with the threading magnetic flux, as long as the system acquires a spatial inversion symmetry. When spatial asymmetry is introduced particle-hole symmetry assures that nonlinear conductance terms maintain certain symmetries with respect to magnetic field and gate voltage. These analytic results are supported by numerical simulations. Analogous results are obtained for the electron heat current. We also demonstrate that a double-dot Aharonov-Bohm interferometer acts as a rectifier when two conditions are met: (i) many-body effects are included, here in the form of inelastic scattering, and (ii) time reversal symmetry is broken.

PACS numbers: 73.23.-b, 85.65.+h, 73.63.-b

## I. INTRODUCTION

Phase-breaking and energy dissipation processes arise due to the interaction of electrons with other degrees of freedom, e.g., with electrons, phonons, and defects. While an understanding of such effects, from first principles, is the desired objective of numerous computational approaches<sup>1</sup>, simple analytical treatments are advantageous as they allow one to gain insights into transport phenomenology. The markovian quantum master equation and its variants (Lindblad, Redfield) is simple to study and interpret<sup>2</sup>, and as such it has been extensively adopted in studies of charge, spin, exciton, and heat transport. It can be derived systematically, from projection operator techniques<sup>3</sup>, and phenomenologically by introducing damping terms into the matrix elements of the reduced density matrix, to include dephasing and inelastic processes into the otherwise coherent dynamics.

Büttiker's probe technique<sup>4-6</sup> and its modern extensions to thermoelectric problems<sup>7-10</sup>, atomic-level thermometry<sup>11</sup>, and beyond linear response situations<sup>12-15</sup> procure an alternative route for introducing decoherence and inelastic processes into coherent conductors. The probe is an electronic component<sup>16</sup>, and it allows one to obtain information about local variables, chemical potential and temperature, deep within the conductor. When coupled strongly to the system, the probe can alter intrinsic transport mechanisms.

Probes can be constructed to induce distinct effects: *Elastic dephasing* processes are implemented by incorporating a “dephasing” probe, enforcing the requirement

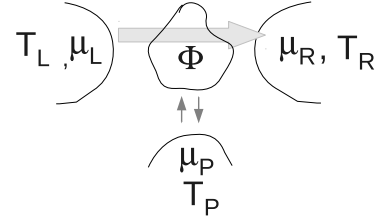


FIG. 1: Scheme of our setup. The horizontal arrow stands for the charge current across the conductor. The two parallel arrows represent currents into and from the  $P$  terminal, serving to induce elastic, inelastic, and dissipative effects. The parameters of the probe  $\mu_P$  and  $T_P$  are determined in a self consistent manner, to satisfy the respective probe condition.

that the net charge current towards the probe terminal, at any given energy, vanishes<sup>17,18</sup>. Inelastic *heat dissipative* effects are included by a voltage probe, by demanding that the total-net charge current to the probe terminal nullifies<sup>4-6</sup>. This process dissipates heat since electrons leaving the system to the probe re-enter the conductor after being thermalized. In the complementary temperature probe *charge dissipation* is allowed at the probe, but the probe temperature is tuned such that the net heat current at the probe is annulled<sup>19</sup>. The voltage-temperature probe, also referred to as a “thermometer”, requires both charge current and heat current at the

probe to vanish. In this case inelastic - energy exchange effects are allowed on the probe, but heat dissipation and charge dissipation effects are excluded.

The probe technique has been used in different applications, particularly for the exploration of the ballistic to diffusive (Ohm's law and Fourier's law) crossover in electronic<sup>5,20</sup> and phononic conductors<sup>21-23</sup>. More recently, the effect of thermal rectification has been studied in phononic systems by utilizing the temperature probe as a mean to incorporate effective anharmonicity<sup>12,13,24</sup>. A full-counting statistics analysis of conductors including dephasing and voltage probes has been carried out in Ref.<sup>25</sup> The probe parameters, temperature and chemical potential, can be derived analytically when the conductor is set close to equilibrium<sup>4,7,16</sup>. Far-from-equilibrium, while these parameters can be technically defined and their uniqueness<sup>14</sup> allows for a physical interpretation, an exact analytic solution is missing. However, recent studies have demonstrated that iterative numerical schemes can reach a stable solution for the temperature probe<sup>13,15</sup>. These techniques have been then used for following phononic heat transfer in the deep quantum limit, far-from-equilibrium<sup>13,15</sup>.

The Onsager-Casimir symmetry relations<sup>26</sup> are satisfied in phase-coherent conductors, reflecting the microreversibility of the scattering matrix. In Aharonov-Bohm interferometers with conserved electron current this symmetry is displayed by the "phase rigidity" of the (linear) conductance oscillations with the magnetic field  $B$ ,  $G_1(B) = G_1(-B)$ <sup>27,28</sup>. Beyond linear response, the phase symmetry of the conductance is not enforced, and several experiments<sup>29,30,32-37</sup> have demonstrated its breakdown. Supporting theoretical works have elucidated the role of many-body interactions in the system<sup>38-42</sup>, typically approaching the problem by calculating the screening potential within the conductor in a self-consistent manner, a procedure often limited to low-order conduction terms<sup>38,40,41</sup>.

The present manuscript is focused on the application of the probe technique to quantum open system problems, possibly in far-from-equilibrium situations. We adopt different probes and consider the role of elastic dephasing, heat dissipation, and charge dissipation processes on magnetic field, temperature bias, and voltage bias symmetries of charge current, rectification, and heat current in Aharonov-Bohm (AB) interferometers. Our main objective is the development, and analysis of the breakdown, of symmetry relations for nonlinear transport beyond the Onsager-Casimir limit, in the presence incoherent effects.

This work extends our recent study<sup>43</sup> in several ways: (i) We consider four different probes (dephasing, voltage, temperature and voltage-temperature) and demonstrate with numerical simulations a stable solution for the probe parameters and a facile convergence, far-from-equilibrium. (ii) We then consider a generic model for an AB interferometer, susceptible to elastic and inelastic effects, and study its conductance behavior: (ii.a) We

provide a detailed proof for the validity of phase rigidity under the voltage probe in the linear response regime. (ii.b) We prove the development of new-general set of magnetic-field symmetry relations away from linear response when the device is geometrically symmetric. (ii.c) These magnetic-field symmetries are invalidated under spatial asymmetry, but we prove that generalized magnetic field-gate voltage symmetry relations are obeyed, a result of particle-hole symmetry. (ii.d) We discuss the operation of the double-dot interferometer, susceptible to inelastic effects, as a charge rectifier, when time reversal symmetry is broken.

The paper is organized as follows. In Sec. II we provide expressions for the charge and heat currents in the Landauer formalism and discuss four types of probes, inducing different effects. Sec. III introduces the main observables of interest and summarizes our principal results. Sec. IV covers setups that fulfill phase rigidity. Magnetic field symmetry relations in a spatially symmetric setup are derived in Sec. V. Magnetic field-gate voltage symmetries, valid for generic double-dot AB interferometer models, are presented in Sec. VI. Supporting numerical simulations are included in Sec. VII. Sec. VIII concludes. For simplicity, we set  $e=1$ ,  $\hbar = 1$  and  $k_B = 1$ . The words "diode" and "rectifier" are used interchangeably in this work, referring to a dc-rectifier.

## II. FORMALISM

In the scattering formalism of Landauer and Büttiker<sup>4,44-46</sup> interactions between particles are neglected. One can then express the charge current from the  $\nu$  to the  $\xi$  terminal in terms of the transmission probability  $\mathcal{T}_{\nu,\xi}(\epsilon)$ , a function which depends on the energy of the incident electron,

$$I_\nu(\phi) = \int_{-\infty}^{\infty} d\epsilon \left[ \sum_{\xi \neq \nu} \mathcal{T}_{\nu,\xi}(\epsilon, \phi) f_\nu(\epsilon) - \sum_{\xi \neq \nu} \mathcal{T}_{\xi,\nu}(\epsilon, \phi) f_\xi(\epsilon) \right]. \quad (1)$$

The magnetic field is introduced via an Aharonov-Bohm flux  $\Phi$  applied through the conductor, with the magnetic phase  $\phi = 2\pi\Phi/\Phi_0$ ,  $\Phi_0 = h/e$  is the magnetic flux quantum. The transmission function can be written in terms of the Green's function of the system and the self energy matrices. Explicit expressions for a particular model are included in Sec. VI. The Fermi-Dirac distribution function  $f_\nu(\epsilon) = [e^{\beta_\nu(\epsilon - \mu_\nu)} + 1]^{-1}$  is defined in terms of the chemical potential  $\mu_\nu$  and the inverse temperature  $\beta_\nu$ .

Our analysis below relies on two basic relations. First, the transmission coefficient from the  $\xi$  to the  $\nu$  reservoir obeys reciprocity, given the unitarity and time reversal symmetry of the scattering matrix,

$$\mathcal{T}_{\xi,\nu}(\epsilon, \phi) = \mathcal{T}_{\nu,\xi}(\epsilon, -\phi). \quad (2)$$

Second, the total probability is conserved,

$$\sum_{\xi \neq \nu} \mathcal{T}_{\xi, \nu}(\epsilon, \phi) = \sum_{\xi \neq \nu} \mathcal{T}_{\nu, \xi}(\epsilon, \phi). \quad (3)$$

A proof for the second relation, in the presence of a probe, is included in Appendix A of Ref.<sup>41</sup>, based on the Green's function formalism.

In this work we consider a setup including three terminals,  $L$ ,  $R$  and  $P$ , where the  $P$  terminal serves as the probe, see Fig. 1. We focus below on the steady-state charge current from the  $L$  reservoir to the central system ( $I_L$ ) and from the probe to the system ( $I_P$ ),

$$I_L(\phi) = \int_{-\infty}^{\infty} d\epsilon \left[ \mathcal{T}_{L,R}(\epsilon, \phi) f_L(\epsilon) - \mathcal{T}_{R,L}(\epsilon, \phi) f_R(\epsilon) + \mathcal{T}_{L,P}(\epsilon, \phi) f_L(\epsilon) - \mathcal{T}_{P,L}(\epsilon, \phi) f_P(\epsilon, \phi) \right], \quad (4)$$

$$I_P(\phi) = \int_{-\infty}^{\infty} d\epsilon \left[ \mathcal{T}_{P,L}(\epsilon, \phi) f_P(\epsilon, \phi) - \mathcal{T}_{L,P}(\epsilon, \phi) f_L(\epsilon) + \mathcal{T}_{P,R}(\epsilon, \phi) f_P(\epsilon, \phi) - \mathcal{T}_{R,P}(\epsilon, \phi) f_R(\epsilon) \right]. \quad (5)$$

Similarly, we can write the heat current at the  $\nu = L$  terminal as

$$Q_L(\phi) = \int_{-\infty}^{\infty} d\epsilon (\epsilon - \mu_L) \left[ \mathcal{T}_{L,R}(\epsilon, \phi) f_L(\epsilon) - \mathcal{T}_{R,L}(\epsilon, \phi) f_R(\epsilon) + \mathcal{T}_{L,P}(\epsilon, \phi) f_L(\epsilon) - \mathcal{T}_{P,L}(\epsilon, \phi) f_P(\epsilon, \phi) \right]. \quad (6)$$

The probe heat current follows an analogous form. The probe distribution function is determined by the probe condition. It is generally affected by the magnetic flux, as we demonstrate in Secs. IV-VII.

For convenience, we simplify next our notation. First, we drop the reference to the energy of incoming electrons  $\epsilon$  in both transmission functions and distribution functions. Second, since all integrals are evaluated between  $\pm\infty$ , we do not put the limits explicitly. Third, unless otherwise mentioned  $f_P$ ,  $\mu_P$  and all transmission coefficients are evaluated at the phase  $+\phi$ , thus we do not explicitly write the phase variable. If we do need to consider e.g. the transmission function  $\mathcal{T}_{\nu, \xi}(-\phi)$ , we write instead the complementary expression,  $\mathcal{T}_{\xi, \nu}(\phi)$ .

*Dephasing probe.* We implement elastic dephasing effects by demanding that the energy-resolved particle current diminishes in the probe,

$$I_P(\epsilon) = 0 \quad \text{with} \quad I_P = \int I_P(\epsilon) d\epsilon. \quad (7)$$

Using this condition, Eq. (5) provides a closed form for the corresponding (flux-dependent) probe distribution, not necessarily in the form of a Fermi function.

*Voltage probe.* We introduce dissipative inelastic effects into the conductor using the voltage probe technique. The three reservoirs are maintained at the same

inverse temperature  $\beta_a$ , but the  $L$  and  $R$  chemical potentials are made distinct,  $\mu_L \neq \mu_R$ . Our objective is to obtain  $\mu_P$ , and it is reached by demanding that the net-total particle current flowing into the  $P$  reservoir diminishes,

$$I_P = 0. \quad (8)$$

This choice allows for dissipative energy exchange processes to take place within the probe. In the linear response regime Eq. (5) can be used to derive an analytic expression for  $\mu_P$ . In far-from-equilibrium situations we obtain the unique<sup>14</sup> chemical potential of the probe numerically, using the Newton-Raphson method<sup>47</sup>

$$\mu_P^{(k+1)} = \mu_P^{(k)} - I_P(\mu_P^{(k)}) \left[ \frac{\partial I_P(\mu_P^{(k)})}{\partial \mu_P} \right]^{-1}. \quad (9)$$

The current  $I_P(\mu_P^{(k)})$  and its derivative are evaluated from Eq. (5) using the probe (Fermi) distribution with  $\mu_P^{(k)}$ . Note that the self-consistent probe solution varies with the magnetic phase.

*Temperature probe.* In this scenario the three reservoirs  $L, R, P$  are maintained at the same chemical potential  $\mu_a$ , but the temperature at the  $L$  and  $R$  terminals vary,  $T_L \neq T_R$ . The probe temperature  $T_P = \beta_P^{-1}$  is determined by requiring the net heat current at the probe to satisfy

$$Q_P = 0. \quad (10)$$

This constraint allows for charge dissipation into the probe since we do not require Eq. (8) to hold. We can obtain the temperature  $T_P$  numerically by following an iterative procedure,

$$T_P^{(k+1)} = T_P^{(k)} - Q_P(T_P^{(k)}) \left[ \frac{\partial Q_P(T_P^{(k)})}{\partial T_P} \right]^{-1}. \quad (11)$$

The probe temperature depends on the flux  $\phi$ , see Appendix B.

*Voltage-temperature probe.* This probe acts as an electron thermometer at weak coupling. We set the temperatures  $T_{L,R}$  and the potentials  $\mu_{L,R}$ , and demand that

$$I_P = 0 \quad \text{and} \quad Q_P = 0. \quad (12)$$

In other words, the charge and heat currents in the conductor satisfy  $I_L = -I_R$  and  $Q_L = -Q_R$ , since neither charge nor heat are allowed to dissipate at the probe. Analytic results can be obtained in the linear response regime, see for example Refs.<sup>7,20</sup>. Beyond that equation (12) can be solved self-consistently, to provide  $T_P$  and  $\mu_P$ . This can be done by utilizing the two-dimensional Newton-Raphson method,

$$\begin{aligned} \mu_P^{(k+1)} &= \mu_P^{(k)} - D_{1,1}^{-1} I_P(\mu_P^{(k)}, T_P^{(k)}) - D_{1,2}^{-1} Q_P(\mu_P^{(k)}, T_P^{(k)}) \\ T_P^{(k+1)} &= T_P^{(k)} - D_{2,1}^{-1} I_P(\mu_P^{(k)}, T_P^{(k)}) - D_{2,2}^{-1} Q_P(\mu_P^{(k)}, T_P^{(k)}), \end{aligned} \quad (13)$$

where the Jacobean  $D$  is re-evaluated at every iteration,

$$D(\mu_P, T_P) \equiv \begin{pmatrix} \frac{\partial I_P(\mu_P, T_P)}{\partial \mu_P} & \frac{\partial I_P(\mu_P, T_P)}{\partial T_P} \\ \frac{\partial Q_P(\mu_P, T_P)}{\partial \mu_P} & \frac{\partial Q_P(\mu_P, T_P)}{\partial T_P} \end{pmatrix}$$

We emphasize that besides the dephasing probe, the function  $f_P(\phi)$  is assumed to take the form of a Fermi-Dirac distribution function.

### III. SYMMETRY MEASURES AND MAIN RESULTS

In the main body of this paper we restrict ourselves to voltage-biased junctions,  $\mu_L \neq \mu_R$ , while setting  $T_a = \beta_a^{-1} = T_L = T_R$ . We also limit our focus to charge conserving systems satisfying

$$I(\phi) \equiv I_L(\phi) = -I_R(\phi), \quad (14)$$

and study the role of elastic dephasing (dephasing probe) and dissipative (voltage probe) and non-dissipative (voltage-temperature probe) inelastic effects on the charge transport symmetries with magnetic flux. In Appendix B we complement this analysis by considering a temperature-biased heat-conserving junction,  $T_L \neq T_R$ ,  $\mu_a = \mu_L = \mu_R$  and  $Q_L = -Q_R$ . We then study the phase symmetry of the heat current, allowing for charge dissipation. Thermoelectric effects are not considered in this work.

We now define several measures for quantifying phase symmetry in a voltage-biased three-terminal junction satisfying Eq. (14). Expanding the charge current in powers of the bias  $\Delta\mu$  we write<sup>48</sup>

$$I(\phi) = G_1(\phi)\Delta\mu + G_2(\phi)(\Delta\mu)^2 + G_3(\phi)(\Delta\mu)^3 + \dots (15)$$

with  $G_{n>1}$  as the nonlinear conductance coefficients. In this work we study relations between two quantities: a measure for the magnetic field asymmetry

$$\Delta I(\phi) \equiv \frac{1}{2}[I(\phi) - I(-\phi)], \quad (16)$$

and the dc-rectification current,

$$\begin{aligned} \mathcal{R}(\phi) &\equiv \frac{1}{2}[I(\phi) + \bar{I}(\phi)] \\ &= G_2(\phi)(\Delta\mu)^2 + G_4(\phi)(\Delta\mu)^4 + \dots \end{aligned} \quad (17)$$

with  $\bar{I}$  defined as the current obtained upon interchanging the chemical potentials of the two terminals. We also study the behavior of odd conductance terms,

$$\begin{aligned} \mathcal{D}(\phi) &\equiv \frac{1}{2}[I(\phi) - \bar{I}(\phi)] \\ &= G_1(\phi)\Delta\mu + G_3(\phi)(\Delta\mu)^3 + \dots \end{aligned} \quad (18)$$

For a non-interacting system we expect the relation

$$I(\phi) = -\bar{I}(-\phi) \quad (19)$$

to hold. Combined with Eq. (15) we immediately note that  $G_{2n+1}(\phi) = G_{2n+1}(-\phi)$  and  $G_{2n}(\phi) = -G_{2n}(-\phi)$  with  $n$  as an integer. We show below that these relations are obeyed in a symmetric junction even when many-body interactions (inelastic scattering) are included. This result is not trivial since the included many-body interactions are reflected by probe parameters which depend on the applied bias in a nonlinear manner and the magnetic phase in an asymmetric form, thus, we cannot assume Eq. (19) to immediately hold.

Using Eq. (4), we express the deviation from the magnetic field symmetry as

$$\begin{aligned} \Delta I &= \frac{1}{2} \int [\mathcal{T}_{L,R} - \mathcal{T}_{R,L}] (f_L + f_R) d\epsilon \\ &+ \frac{1}{2} \int [\mathcal{T}_{L,P} - \mathcal{T}_{P,L}] f_L d\epsilon \\ &+ \frac{1}{2} \int [\mathcal{T}_{L,P} f_P(-\phi) - \mathcal{T}_{P,L} f_P(\phi)] d\epsilon \end{aligned} \quad (20)$$

We use the probability conservation, Eq. (3), and simplify this relation,

$$\begin{aligned} \Delta I &= \frac{1}{2} \int [\mathcal{T}_{L,R} - \mathcal{T}_{R,L}] f_R d\epsilon \\ &+ \frac{1}{2} \int [\mathcal{T}_{L,P} f_P(-\phi) - \mathcal{T}_{P,L} f_P(\phi)] d\epsilon. \end{aligned} \quad (21)$$

The rectification current can be written as

$$\mathcal{R} = \int \frac{\mathcal{T}_{P,L} - \mathcal{T}_{P,R}}{4} (f_L + f_R - f_P(\phi) - \bar{f}_P(\phi)) d\epsilon \quad (22)$$

with  $\bar{f}_P$  as the probe distribution when the biases  $\mu_L$  and  $\mu_R$  are interchanged.

Our results are organized by systematically departing from quantum coherent scenarios, the linear response regime, and spatially symmetric situations. The paper includes four parts, and we now summarize our main results:

(i) *Phase Rigidity.* In Sec. IV we discuss two scenarios that do obey the Onsager-Casimir symmetry relation  $I(\phi) = I(-\phi)$ : It is maintained in the presence of elastic dephasing effects even beyond linear response. This relation is also valid when inelastic scatterings are included, albeit only in the linear response regime. While these results are not new<sup>45</sup>, we include this analysis here so as to clarify the role of inelastic effects in breaking the Onsager symmetry, beyond linear response.

(ii) *Magnetic field (MF) symmetry relations beyond linear response.* In Sec. V we derive magnetic-field symmetry relations that hold far-from-equilibrium in *spatially symmetric* junctions susceptible to inelastic effects,  $\mathcal{R}(\phi) = \Delta I(\phi) = -\mathcal{R}(-\phi)$  and  $\mathcal{D}(\phi) = \mathcal{D}(-\phi)$ . In other words, we show that odd (even) conductance terms are even (odd) in the magnetic flux. Note that ‘‘spatial’’ or ‘‘geometrical’’ symmetry refers here to the left-right mirror symmetry of the junction. Below we refer to these symmetries as the ‘‘MF symmetry relations’’.

(iii) *Magnetic field-Gate voltage (MFGV) symmetry relations beyond linear response.* In Secs. VI-VII we focus on geometrically *asymmetric* setups, adopting the double dot AB interferometer as an example. While we demonstrate, using numerical simulations, the breakdown of the MF relations under spatial asymmetry, in Appendix A we prove that charge conjugation symmetry entails magnetic field-gate voltage symmetries:  $\mathcal{R}(\epsilon_d, \phi) = -\mathcal{R}(-\epsilon_d, -\phi)$ , and  $\mathcal{D}(-\epsilon_d, -\phi) = \mathcal{D}(\epsilon_d, \phi)$ , with  $\epsilon_d$  as the double-dot energies. We refer below to these symmetries as the ‘‘MFGV symmetry relations’’.

(iv) In Appendix B we prove that the heat current (within a heat-conserving setup) satisfies relations analogous to (i)-(iii).

#### IV. PHASE RIGIDITY AND ABSENCE OF RECTIFICATION

The Onsager-Casimir symmetry  $I(\phi) = I(-\phi)$  is preserved under dephasing effects, implemented via a dephasing probe, even beyond the linear response regime. It is also satisfied in the presence of elastic and inelastic effects, implemented using the voltage probe technique, only as long as the system is maintained in the linear response regime. These results have already been discussed in e.g., Ref.<sup>45</sup>. We details these steps here so as to provide closed expressions for the probe parameters in the linear response regime.

##### A. Dephasing effects beyond linear response

Implementing the dephasing probe (7) we obtain the respective distribution

$$f_P(\phi) = \frac{\mathcal{T}_{L,P}f_L + \mathcal{T}_{R,P}f_R}{\mathcal{T}_{P,L} + \mathcal{T}_{P,R}}. \quad (23)$$

We substitute this function into Eq. (21), a measure for phase asymmetry, and obtain

$$\begin{aligned} \Delta I &= \frac{1}{2} \int [\mathcal{T}_{L,R} - \mathcal{T}_{R,L}] f_R d\epsilon \\ &+ \frac{1}{2} \int \mathcal{T}_{L,P} \frac{\mathcal{T}_{P,L}f_L + \mathcal{T}_{P,R}f_R}{\mathcal{T}_{L,P} + \mathcal{T}_{R,P}} d\epsilon \\ &- \frac{1}{2} \int \mathcal{T}_{P,L} \frac{\mathcal{T}_{L,P}f_L + \mathcal{T}_{R,P}f_R}{\mathcal{T}_{P,L} + \mathcal{T}_{P,R}} d\epsilon \end{aligned} \quad (24)$$

The denominators in these integrals are identical, see Eq. (3), thus we combine the last two terms

$$\begin{aligned} \Delta I &= \frac{1}{2} \int [\mathcal{T}_{L,R} - \mathcal{T}_{R,L}] f_R d\epsilon \\ &+ \frac{1}{2} \int \frac{[\mathcal{T}_{L,P}\mathcal{T}_{P,R} - \mathcal{T}_{P,L}\mathcal{T}_{R,P}] f_R}{\mathcal{T}_{P,R} + \mathcal{T}_{P,L}} d\epsilon \end{aligned} \quad (25)$$

Utilizing Eq. (3) in the form  $\mathcal{T}_{L,P} = \mathcal{T}_{P,L} + \mathcal{T}_{P,R} - \mathcal{T}_{R,P}$ , we organize the numerator of the second integral, ( $\mathcal{T}_{P,R} -$

$\mathcal{T}_{R,P}$ )( $\mathcal{T}_{P,R} + \mathcal{T}_{P,L}$ ) $f_R$ . This results in

$$\begin{aligned} \Delta I &= \frac{1}{2} \int [\mathcal{T}_{L,R} - \mathcal{T}_{R,L} + \mathcal{T}_{P,R} - \mathcal{T}_{R,P}] f_R d\epsilon \\ &= \frac{1}{2} \int f_R \left[ \sum_{\nu \neq R} \mathcal{T}_{\nu,R} - \sum_{\nu \neq R} \mathcal{T}_{R,\nu} \right] d\epsilon, \end{aligned} \quad (26)$$

which is identically zero, given Eq. (3). This concludes our proof that dephasing effects, implemented via a dephasing probe, cannot break phase rigidity even in the nonlinear regime.

Following similar steps we show that elastic dephasing effects cannot generate the effect of charge rectification even when the junction acquires spatial asymmetries. We substitute  $f_P$  into Eq. (4) and obtain

$$I_L = \int [F_L f_L - F_R f_R] d\epsilon \quad (27)$$

with

$$F_L = \frac{\mathcal{T}_{L,R}(\mathcal{T}_{P,L} + \mathcal{T}_{P,R}) + \mathcal{T}_{L,P}\mathcal{T}_{P,R}}{(\mathcal{T}_{P,L} + \mathcal{T}_{P,R})}. \quad (28)$$

$F_R$  is defined analogously, interchanging  $L$  by  $R$ . We now note the following identities,

$$\begin{aligned} \mathcal{T}_{L,P}\mathcal{T}_{P,R} &= [\mathcal{T}_{P,L} + \mathcal{T}_{P,R} - \mathcal{T}_{R,P}]\mathcal{T}_{P,R} \\ &= (\mathcal{T}_{P,R} - \mathcal{T}_{R,P})(\mathcal{T}_{P,R} + \mathcal{T}_{P,L}) + \mathcal{T}_{P,L}\mathcal{T}_{R,P} \\ &= (\mathcal{T}_{R,L} - \mathcal{T}_{L,R})(\mathcal{T}_{P,R} + \mathcal{T}_{P,L}) + \mathcal{T}_{P,L}\mathcal{T}_{R,P} \end{aligned} \quad (29)$$

Reorganizing the first and third lines we find that

$$\begin{aligned} \mathcal{T}_{L,R}(\mathcal{T}_{P,R} + \mathcal{T}_{P,L}) + \mathcal{T}_{L,P}\mathcal{T}_{P,R} \\ = \mathcal{T}_{R,L}(\mathcal{T}_{P,R} + \mathcal{T}_{P,L}) + \mathcal{T}_{P,L}\mathcal{T}_{R,P} \end{aligned} \quad (30)$$

which immediately implies that  $F_L = F_R$ . This in turn leads to  $I = -I$ , thus  $\mathcal{R} = 0$ . We conclude that the current only includes odd (linear and nonlinear) conductance terms under elastic dephasing,  $I = \mathcal{D}(\phi) = \mathcal{D}(-\phi)$ , and that phase rigidity is maintained even if spatial asymmetry is presented. This conclusion is valid under either a voltage or a temperature bias.

##### B. Inelastic effects in linear response

We introduce inelastic effects using the voltage probe technique. In the linear response regime we expand the  $\nu = L, R, P$  Fermi functions around the equilibrium state  $f_a(\epsilon) = [e^{\beta a(\epsilon - \mu_a)} + 1]^{-1}$ ,

$$f_\nu(\epsilon) = f_a(\epsilon) - (\mu_\nu - \mu_a) \frac{\partial f_a}{\partial \epsilon}. \quad (31)$$

The three terminals are maintained at the same temperature  $T_a$ . The derivative  $\frac{\partial f_a}{\partial \epsilon}$  is evaluated at the equilibrium value  $\mu_a$ . For simplicity we set  $\mu_a = 0$ . We enforce the voltage probe condition,  $I_P = 0$ , demanding that

$$\int [(\mathcal{T}_{P,L} + \mathcal{T}_{P,R}) f_P(\phi) - \mathcal{T}_{L,P}f_L - \mathcal{T}_{R,P}f_R] d\epsilon = 0. \quad (32)$$

In linear response this translates to

$$0 = \int \left[ (\mathcal{T}_{P,L} + \mathcal{T}_{P,R}) \left( f_a - \mu_P(\phi) \frac{\partial f_a}{\partial \epsilon} \right) - \mathcal{T}_{L,P} \left( f_a - \mu_L \frac{\partial f_a}{\partial \epsilon} \right) - \mathcal{T}_{R,P} \left( f_a - \mu_R \frac{\partial f_a}{\partial \epsilon} \right) \right] d\epsilon. \quad (33)$$

For convenience, we apply the voltage symmetrically,  $\mu_L = -\mu_R = \Delta\mu/2$ . We organize Eq. (33) and obtain the probe chemical potential, a linear function in  $\Delta\mu$ ,

$$\mu_P(\phi) = \frac{\Delta\mu \int d\epsilon \frac{\partial f_a}{\partial \epsilon} (\mathcal{T}_{L,P} - \mathcal{T}_{R,P})}{2 \int d\epsilon \frac{\partial f_a}{\partial \epsilon} (\mathcal{T}_{P,L} + \mathcal{T}_{P,R})}. \quad (34)$$

We simplify this result by introducing a short notation for the conductance between the  $\nu$  and  $\xi$  terminals,

$$G_{\nu,\xi}(\phi) \equiv \int d\epsilon \left( -\frac{\partial f_a}{\partial \epsilon} \right) \mathcal{T}_{\nu,\xi}(\epsilon, \phi). \quad (35)$$

This quantity fulfills relations analogous to Eqs. (2) and (3)<sup>4</sup>. For brevity, we do not write next the phase variable in  $G$ , evaluating it at the phase  $\phi$  unless otherwise mentioned. The probe potential can now be compacted,

$$\mu_P(\phi) = \frac{\Delta\mu G_{L,P} - G_{R,P}}{2 G_{P,L} + G_{P,R}}. \quad (36)$$

Furthermore, in geometrically symmetric systems  $\mathcal{T}_{R,P}(\epsilon, \phi) = \mathcal{T}_{P,L}(\epsilon, \phi)$ , resulting in  $G_{R,P}(\phi) = G_{P,L}(\phi)$  and

$$\mu_P(\phi) = \frac{\Delta\mu G_{L,P}(\phi) - G_{L,P}(-\phi)}{2 G_{L,P}(\phi) + G_{L,P}(-\phi)}. \quad (37)$$

Thus  $\mu_P(\phi) = -\mu_P(-\phi)$  in linear response. Below we show that this symmetry does not hold far-from-equilibrium. We now expand Eq. (21) in the linear response regime

$$\begin{aligned} \Delta I &= \frac{1}{2} \int (\mathcal{T}_{L,R} - \mathcal{T}_{R,L}) \left( f_a - \mu_R \frac{\partial f_a}{\partial \epsilon} \right) d\epsilon \\ &+ \frac{1}{2} \int \left\{ \mathcal{T}_{L,P} \left[ f_a - \mu_P(-\phi) \frac{\partial f_a}{\partial \epsilon} \right] - \mathcal{T}_{P,L} \left[ f_a - \mu_P(\phi) \frac{\partial f_a}{\partial \epsilon} \right] \right\} d\epsilon. \end{aligned} \quad (38)$$

Utilizing the definition (35) we compact this expression,

$$\begin{aligned} \Delta I &= \frac{1}{2} (G_{L,R} - G_{R,L}) (\mu_R) \\ &- \frac{1}{2} [G_{P,L} \mu_P(\phi) - G_{L,P} \mu_P(-\phi)]. \end{aligned} \quad (39)$$

Using Eq. (3), the first line can be rewritten as

$$I_1 = \frac{\Delta\mu}{4} (G_{L,P} - G_{P,L}). \quad (40)$$

The second line in Eq. (39) reduces to

$$\begin{aligned} I_2 &= -\frac{\Delta\mu}{4} G_{P,L} \frac{G_{L,P} - G_{R,P}}{\mathcal{N}} + \frac{\Delta\mu}{4} G_{L,P} \frac{G_{P,L} - G_{P,R}}{\mathcal{N}} \\ &= -\frac{\Delta\mu}{4} \frac{G_{L,P} G_{P,R} - G_{P,L} G_{R,P}}{\mathcal{N}} \end{aligned} \quad (41)$$

where we have introduced the short notation  $\mathcal{N} \equiv G_{P,L} + G_{P,R}$ . Now, we substitute  $G_{L,P} = G_{P,L} + G_{P,R} - G_{R,P}$ , and this allows us to write

$$\begin{aligned} I_2 &= -\frac{\Delta\mu}{4} \frac{(G_{P,R} - G_{R,P})(G_{P,R} + G_{P,L})}{\mathcal{N}} \\ &= -\frac{\Delta\mu}{4} (G_{P,R} - G_{R,P}) \end{aligned} \quad (42)$$

Combining  $\Delta I = I_1 + I_2$ , we reach

$$\begin{aligned} \Delta I &= -\frac{\Delta\mu}{4} (G_{P,R} - G_{R,P} - G_{L,P} + G_{P,L}) \\ &= -\frac{\Delta\mu}{4} \left( \sum_{\nu \neq P} G_{P,\nu} - \sum_{\nu \neq P} G_{\nu,P} \right) \end{aligned} \quad (43)$$

which is identically zero given the conductance conservation (3). It is trivial to note that no rectification takes place in the linear response regime,  $\mathcal{R} = 0$ .

## V. BEYOND LINEAR RESPONSE: SPATIALLY SYMMETRIC SETUPS

In this section we consider the role of inelastic effects on the current symmetry in an AB interferometer, beyond the linear response regime. The probe condition  $I_P = 0$  translates Eq. (5) into three relations,

$$\begin{aligned} \int d\epsilon (\mathcal{T}_{P,L} + \mathcal{T}_{P,R}) f_P(\phi) &= \int d\epsilon (\mathcal{T}_{L,P} f_L + \mathcal{T}_{R,P} f_R) \\ \int d\epsilon (\mathcal{T}_{L,P} + \mathcal{T}_{R,P}) f_P(-\phi) &= \int d\epsilon (\mathcal{T}_{P,L} f_L + \mathcal{T}_{P,R} f_R) \\ \int d\epsilon (\mathcal{T}_{P,L} + \mathcal{T}_{P,R}) \bar{f}_P(\phi) &= \int d\epsilon (\mathcal{T}_{L,P} f_R + \mathcal{T}_{R,P} f_L) \end{aligned} \quad (44)$$

First, we consider the situation when time reversal symmetry is protected with the magnetic phase given by multiples of  $2\pi$ . Then,  $\mathcal{T}_{\nu,\xi} = \mathcal{T}_{\xi,\nu}$ , and particularly we note that  $\mathcal{T}_{L,P} = \mathcal{T}_{P,L}$ . Furthermore, in the model considered in Sec. VI,  $\mathcal{T}_{P,L} = \chi \mathcal{T}_{P,R}$ , with  $\chi$  as an energy independent parameter, reflecting spatial asymmetry, see for example the discussion around Eq. (58). Using the voltage probe condition (44) we find that

$$\begin{aligned} &\int (\mathcal{T}_{P,L} + \mathcal{T}_{P,R}) (f_P(\phi) + \bar{f}_P(\phi)) d\epsilon \\ &= \int (\mathcal{T}_{P,L} + \mathcal{T}_{P,R}) (f_L + f_R) d\epsilon, \end{aligned} \quad (45)$$

Given the linear relation between  $\mathcal{T}_{L,P}$  and  $\mathcal{T}_{R,P}$ , this equality holds separately for each transmission function,

$$\begin{aligned} & \int \mathcal{T}_{P,\nu}(f_P(\phi) + \bar{f}_P(\phi))d\epsilon \\ &= \int \mathcal{T}_{P,\nu}(f_L + f_R)d\epsilon \quad \nu = L, R, \end{aligned} \quad (46)$$

providing  $\mathcal{R} = 0$  in Eq. (22). Thus, if  $\mathcal{T}_{P,L} = \mathcal{T}_{L,P} = \chi\mathcal{T}_{P,R}$ , rectification is absent. In physical terms, the junction conducts symmetrically for forward and reversed direction, though many-body effects are presented, if we satisfy two conditions: (i) Spatial asymmetry is included in an energy-independent manner, for example using different broad-band hybridization parameters at the two ends. (ii) Time reversal symmetry is protected.

We now derive symmetry relations for left-right symmetric systems with broken time-reversal symmetry. In this case the mirror symmetry  $\mathcal{T}_{P,L}(\phi) = \mathcal{T}_{P,R}(-\phi)$  applies, translating to

$$\mathcal{T}_{P,L}(\phi) = \mathcal{T}_{R,P}(\phi). \quad (47)$$

When used in Eq. (44), we note that the distributions should obey

$$\bar{f}_P(\phi) = f_P(-\phi), \quad (48)$$

leading to  $\bar{\mu}_P(\phi) = \mu_P(-\phi)$ . We emphasize that  $\mu_P(\phi)$  itself does not possess a phase symmetry.

Since charge dissipation is not allowed, the deviation from phase rigidity, Eq. (21), can be also expressed in terms of the current  $I_R$ , to provide (note the sign convention)

$$\begin{aligned} \Delta I(\phi) &= \frac{1}{2} \int d\epsilon [(\mathcal{T}_{L,R} - \mathcal{T}_{R,L})f_L \\ &\quad - \mathcal{T}_{R,P}f_P(-\phi) + \mathcal{T}_{P,R}f_P(\phi)]. \end{aligned} \quad (49)$$

We define  $\Delta I$  by the average of Eqs. (21) and (49),

$$\begin{aligned} \Delta I(\phi) &= \frac{1}{4} \int d\epsilon [(\mathcal{T}_{L,R} - \mathcal{T}_{R,L})(f_L + f_R) \\ &\quad + (\mathcal{T}_{L,P} - \mathcal{T}_{R,P})f_P(-\phi) + (\mathcal{T}_{P,R} - \mathcal{T}_{P,L})f_P(\phi)]. \end{aligned}$$

We proceed and make use of two relations:  $\mathcal{T}_{L,R} - \mathcal{T}_{R,L} = \mathcal{T}_{P,L} - \mathcal{T}_{L,P}$  and Eq (47), valid in geometrically symmetric junctions. With this at hand we write

$$\begin{aligned} \Delta I(\phi) &= \frac{1}{4} \int (\mathcal{T}_{P,L} - \mathcal{T}_{P,R})(f_L + f_R - f_P(\phi) - \bar{f}_P(\phi))d\epsilon \\ &= \mathcal{R}(\phi) = -\mathcal{R}(-\phi), \end{aligned} \quad (50)$$

This concludes our derivation that

$$\Delta I(\phi) = \mathcal{R}(\phi) = -\mathcal{R}(-\phi), \quad \mathcal{D}(\phi) = \mathcal{D}(-\phi). \quad (51)$$

In spatially symmetric systems odd conductance terms acquire even symmetry with respect to the magnetic

field, as noted experimentally<sup>33,35</sup>, while even conductance terms, constructing  $\mathcal{R}$ , are odd with respect to  $\phi$ . The relation  $\Delta I(\phi) = \mathcal{R}(\phi)$  could be exploited in experimental studies: One could determine whether a quantum dot junction is  $L$ - $R$  symmetric by testing this equality.

The following observations can be made: First, Eq. (51) does not hold when a spatial asymmetry is introduced, by coupling the scattering centers unevenly to the leads. Second, the symmetry relations obtained here are valid under the more restrictive (non-dissipative) voltage-temperature probe, Eq. (12). Finally, the analysis in this section reveals sufficient conditions for charge rectification for structurally *symmetric* junctions:  $\mathcal{R}(\phi) \neq 0$  when time-reversal symmetry is broken,  $\phi \neq 2\pi n$ , and inelastic scatterings are allowed.

## VI. BEYOND LINEAR RESPONSE: SPATIALLY ASYMMETRIC SETUPS

We adopt a double-dot AB model, see Fig. 2, allow for inelastic effects and spatial asymmetry, and prove analytically the validity of magnetic field - gate voltage symmetries.

### A. Model: Double-dot Interferometer

We focus on an AB setup with a quantum dot located at each arm of the interferometer. The dots are connected to two metal leads maintained in a biased state. For simplicity, we do not consider electron-electron interactions and the Zeeman effect, thus, we can ignore the spin degree of freedom and describe each quantum dot by a spinless electronic level. The total Hamiltonian includes the following terms,

$$H = H_S + \sum_{\nu=L,R,P} H_\nu + \sum_{\nu=L,R} H_{S,\nu} + H_{S,P} \quad (52)$$

The subsystem Hamiltonian includes two (uncoupled) electronic states

$$H_S = \sum_{n=1,2} \epsilon_n a_n^\dagger a_n. \quad (53)$$

The three reservoirs (metals) comprise of a collection of non-interacting electrons,

$$H_\nu = \sum_{j \in \nu} \epsilon_j a_j^\dagger a_j. \quad (54)$$

Here  $a_j^\dagger$  ( $a_j$ ) are fermionic creation (annihilation) operators of electrons with momentum  $j$  and energy  $\epsilon_j$ .  $a_n^\dagger$  and  $a_n$  are the respective operators for the dots. The subsystem-bath coupling terms are given by

$$H_{S,L} + H_{S,R} = \sum_{n,l} v_{n,l} a_n^\dagger a_l e^{i\phi_n^L} + \sum_{n,r} v_{n,r} a_r^\dagger a_n e^{i\phi_n^R} + h.c..$$

We assume that only dot '1' couples to the probe

$$H_{S,P} = \sum_p v_{1,p} a_1^\dagger a_p + h.c. \quad (55)$$

Here  $v_{n,j}$  is the coupling strength of dot  $n$  to the  $j$  state of the  $J$  bath. Below we assume that this parameter does not depend on the  $n = 1, 2$  level index.  $\phi_n^L$  and  $\phi_n^R$  are the AB phase factors, acquired by electron waves in a magnetic field perpendicular to the device plane. These phases are constrained to satisfy

$$\phi_1^L - \phi_2^L + \phi_1^R - \phi_2^R = \phi \quad (56)$$

and we adopt the gauge  $\phi_1^L - \phi_2^L = \phi_1^R - \phi_2^R = \phi/2$ .

We voltage-bias the system,  $\Delta\mu \equiv \mu_L - \mu_R$ , with  $\mu_{L,R}$  as the chemical potential of the metals, and use the convention that a positive current is flowing left-to-right. While we bias the system in a symmetric manner,  $\mu_L = -\mu_R$ , this choice does not limit the generality of our discussion since the dots may be gated away from the so called "symmetric point" at which  $\mu_L - \epsilon_n = \epsilon_n - \mu_R$ .

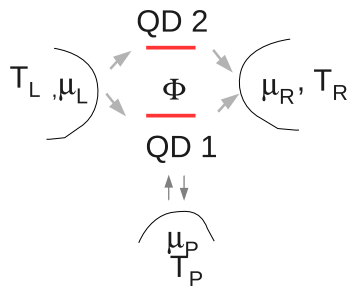


FIG. 2: Scheme of a double-dot AB interferometer susceptible to many-body effects. The two quantum dots (QD) are each represented by a single electronic level, which do not directly couple. The total magnetic flux is denoted by  $\Phi$ . Dot '1' may be susceptible to elastic dephasing and inelastic effects, introduced here through the coupling of this dot to a probe, the terminal  $P$ .

## B. Green's function expressions

Our model does not include interacting particles, thus its steady-state characteristics can be written exactly using the nonequilibrium Green's function approach<sup>49,50</sup>. Transient effects were recently explored in Refs.<sup>51,52</sup>. Since relevant derivations were detailed in our recent study<sup>53</sup>, we only include here the principal expressions. In terms of the Green's function, the transmission coefficient is defined as

$$\mathcal{T}_{\nu,\xi} = \text{Tr}[\Gamma^\nu G^+ \Gamma^\xi G^-], \quad (57)$$

where the trace is performed over the states of the subsystem (dots). In our model the matrix  $G^+$  ( $G^- = [G^+]^\dagger$ ) takes the form

$$G^+ = \begin{bmatrix} \epsilon - \epsilon_1 + \frac{i(\gamma_L + \gamma_R + \gamma_P)}{2} & \frac{i\gamma_L}{2} e^{i\phi/2} + \frac{i\gamma_R}{2} e^{-i\phi/2} \\ \frac{i\gamma_L}{2} e^{-i\phi/2} + \frac{i\gamma_R}{2} e^{i\phi/2} & \epsilon - \epsilon_2 + \frac{i(\gamma_L + \gamma_R)}{2} \end{bmatrix}^{-1},$$

with the hybridization matrices satisfying

$$\Gamma^L = \gamma_L \begin{bmatrix} 1 & e^{i\phi/2} \\ e^{-i\phi/2} & 1 \end{bmatrix}, \quad \Gamma^R = \gamma_R \begin{bmatrix} 1 & e^{-i\phi/2} \\ e^{i\phi/2} & 1 \end{bmatrix} \\ \Gamma^P = \gamma_P \begin{bmatrix} 1 & 0 \\ 0 & 0 \end{bmatrix} \quad (58)$$

The coupling energy between the dots and leads is given by  $\gamma_\nu(\epsilon) = 2\pi \sum_{j \in \nu} |v_j|^2 \delta(\epsilon - \epsilon_j)$ . In the wide-band limit adopted in this work  $\gamma_\nu$  are taken as energy independent parameters.

We now assume that the dots are energy-degenerate,  $\epsilon_d \equiv \epsilon_1 = \epsilon_2$ , but allow for spatial asymmetry in the form  $\gamma_L \neq \gamma_R$ . The transmission functions follow a simple form,

$$\mathcal{T}_{LR} = \frac{\gamma_L \gamma_R}{\Delta(\epsilon, \phi)} \left[ 4(\epsilon - \epsilon_d)^2 \cos^2 \frac{\phi}{2} + \frac{\gamma_P^2}{4} + \gamma_P(\epsilon_d - \epsilon) \sin \phi \right] \\ \mathcal{T}_{LP} = \frac{\gamma_L \gamma_P}{\Delta(\epsilon, \phi)} \left[ (\epsilon - \epsilon_d)^2 + \gamma_R^2 \sin^2 \frac{\phi}{2} + \gamma_R(\epsilon - \epsilon_d) \sin \phi \right] \\ \mathcal{T}_{RP} = \frac{\gamma_R \gamma_P}{\Delta(\epsilon, \phi)} \left[ (\epsilon - \epsilon_d)^2 + \gamma_L^2 \sin^2 \frac{\phi}{2} - \gamma_L(\epsilon - \epsilon_d) \sin \phi \right] \quad (59)$$

with the denominator an even function of  $\phi$ ,

$$\Delta(\epsilon, \phi) = \left[ (\epsilon - \epsilon_d)^2 - \gamma_L \gamma_R \sin^2 \frac{\phi}{2} - \frac{(\gamma_L + \gamma_R) \gamma_P}{4} \right]^2 \\ + \left( \gamma_L + \gamma_R + \frac{\gamma_P}{2} \right)^2 (\epsilon - \epsilon_d)^2. \quad (60)$$

It is trivial to confirm that in the absence of the probe the even symmetry of the current with  $\phi$  is satisfied, beyond linear response<sup>54</sup>.

$$I_L(\phi) = \int d\epsilon \frac{4\gamma_L \gamma_R (\epsilon - \epsilon_d)^2 \cos^2 \frac{\phi}{2} [f_L(\epsilon) - f_R(\epsilon)]}{\left[ (\epsilon - \epsilon_d)^2 - \gamma_L \gamma_R \sin^2 \frac{\phi}{2} \right]^2 + (\gamma_L + \gamma_R)^2 (\epsilon - \epsilon_d)^2}$$

With the probe, inspecting the transmission functions in conjunction with Eq. (36), we immediately conclude that under spatial asymmetries the probe chemical potential does not obey a particular symmetry, even in linear response when phase rigidity is trivially obeyed, see Sec. IV B.

We now discuss the properties of the probe when the interferometer is  $L$ - $R$  symmetric,  $\gamma/2 = \gamma_L = \gamma_R$ . The transmission functions satisfy  $\mathcal{T}_{R,P}(\epsilon, \phi) = \mathcal{T}_{P,L}(\epsilon, \phi)$ . We substitute these expressions into Eq. (23) and resolve the dephasing probe distribution<sup>53</sup>

$$f_P^D(\epsilon, \phi) = \frac{f_L(\epsilon) + f_R(\epsilon)}{2} \\ + \frac{\gamma(\epsilon - \epsilon_d) \sin \phi}{4 \left[ (\epsilon - \epsilon_d)^2 + \omega_0^2 \right]} [f_L(\epsilon) - f_R(\epsilon)] \quad (61)$$

with  $\omega_0 = \frac{\gamma}{2} \sin \frac{\phi}{2}$ . The nonequilibrium term in this distribution is *odd* in the magnetic flux. Similarly, when a voltage probe ( $V$ ) is implemented, analytic results can be obtained in the linear response regime,

$$\mu_P^V(\phi) = \Delta\mu \sin \phi \frac{\int d\epsilon \frac{\partial f_a}{\partial \epsilon} \frac{\gamma(\epsilon - \epsilon_d)}{\Delta(\epsilon, \phi)}}{\int d\epsilon \frac{\partial f_a}{\partial \epsilon} \frac{2(\epsilon - \epsilon_d)^2 + \frac{1}{2}\gamma^2 \sin^2 \frac{\phi}{2}}{\Delta(\epsilon, \phi)}}. \quad (62)$$

Here  $f_a$  stands for the equilibrium (zero bias) Fermi-Dirac function. This chemical potential is an *odd* function of the magnetic flux, though phase rigidity is maintained in the linear response regime.

### C. Generalized magnetic field-gate voltage symmetries

The MF symmetry relations (51) are not obeyed when the spatial mirror symmetry is broken. Instead, in Appendix A we prove that in a generic model for a double-dot interferometer susceptible to inelastic effects the following result holds

$$\mathcal{R} = -\mathcal{C}(\mathcal{R}), \quad \mathcal{D} = \mathcal{C}(\mathcal{D}). \quad (63)$$

Here  $\mathcal{C}$  stands for the charge conjugation operator, transforming electrons to holes and vice versa. In terms of the interferometer parameters this relation reduces to the following magnetic flux-gate voltage (MFGV) symmetries,

$$\begin{aligned} \mathcal{R}(\epsilon_d, \phi) &= -\mathcal{R}(-\epsilon_d, -\phi), \\ \mathcal{D}(\epsilon_d, \phi) &= \mathcal{D}(-\epsilon_d, -\phi). \end{aligned} \quad (64)$$

Since the energies of the dots can be modulated with a gate voltage<sup>37</sup>, these generalized symmetries can be examined experimentally.

## VII. NUMERICAL SIMULATIONS

Using numerical simulations we demonstrate the behavior of the voltage and the voltage-temperature probes far-from-equilibrium, and the implications on phase rigidity and magnetic field symmetries.

### A. Probe parameters

We consider the model Eq. (52) and implement inelastic effects with the dissipative voltage probe, by solving the probe condition (8) numerically-iteratively, using Eq. (9), to obtain  $\mu_P$ . We also investigate the transport behavior of the model under the more restrictive dissipationless voltage-temperature probe, by solving Eq. (13) to obtain both  $\mu_P$  and  $T_P$ .

Fig. 3 displays the self-consistent probe parameters  $\mu_P$  and  $T_P$  for  $\phi = 0$  when heat dissipation is allowed at the probe (full line), and when neither heat nor

charge dissipation takes place within  $P$  (dashed line). We find that the probe parameters largely vary depending on the probe condition, particularly at high biases when significant heat dissipation can take place [panel (d)]. We also verify that when Newton-Raphson iterations converge, the charge current to the probe is negligible,  $|I_P/I_L| < 10^{-12}$ . Similarly, the heat current in the voltage-temperature probe is negligible once convergence is reached.

Uniqueness of the parameters of the voltage and temperature probes has been recently proved in Ref.<sup>14</sup>. We complement this analytical analysis and demonstrate that the parameters of the voltage-temperature probe are insensitive to the initial conditions adopted, see Fig. 4. Convergence has been typically achieved with  $\sim 5$  iterations. While the voltage probe had easily converged even at large biases, we could not manage to converge the voltage-temperature probe parameters at large biases  $\Delta\mu > 1$  and low temperatures  $T_{L,R} < 1/50$  since eliminating heat dissipation within the probe requires extreme values, leading to numerical divergences within the model parameters adopted.

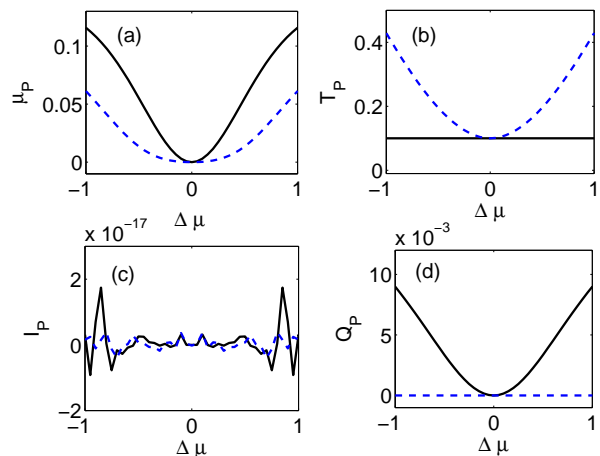


FIG. 3: Self-consistent parameters of the voltage probe (full) and the voltage-temperature probe (dashed), displaying disparate behavior far-from-equilibrium: (a) Probe chemical potential, (b) temperature. We also show (c) the magnitude of net charge current from the probe and (d) net heat current from the conductor towards the probe. The interferometer consists two degenerate levels with  $\epsilon_{1,2} = 0.15$  coupled evenly to the metal leads  $\gamma_{L,R} = 0.05$ . Other parameters are  $\gamma_P = 0.1$ ,  $\phi = 0$ , and  $T_L = T_R = 0.1$ . The probe temperature is set at  $T_P = 0.1$  in the voltage probe case.

### B. Nonlinear transport with dissipative inelastic effects

In this subsection we examine the nonlinear transport behavior of an AB interferometer coupled to a voltage probe. In Fig. 5 (a) we display the measure  $\Delta I$  as a function of bias for a spatially symmetric system using

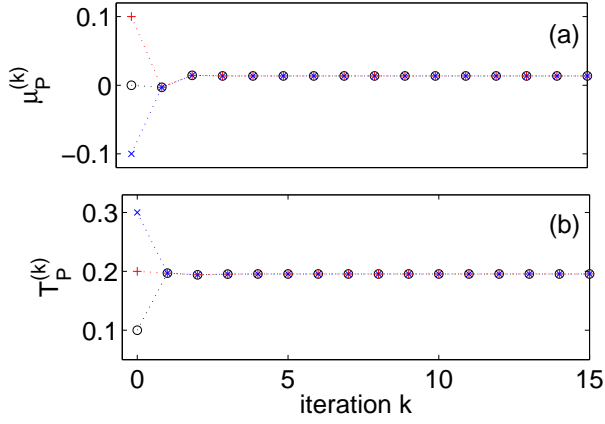


FIG. 4: Insensitivity of the parameters of the voltage-temperature probe [Eq. (13)] to initial conditions. (a) chemical potential of the probe and (b) its temperature. The different initial conditions are identified by the values at the first iteration. The interferometer's parameters follow Fig. 3 with  $\Delta\mu = 0.5$  and  $T_L = T_R = 0.1$ .

two representative phases,  $\phi = \pi/2$  and  $\pi/4$ . We confirm numerically that in the linear response regime  $\Delta I = 0$ . More generally, the relation  $\Delta I = \mathcal{R}$  is satisfied for all biases, as expected from Eq. (51). Our conclusions are intact when an “up-down” asymmetry is implemented in the form  $\epsilon_1 \neq \epsilon_2$ <sup>43</sup>. The corresponding chemical potential of the probe is shown in Fig. 5(b)-(c) for  $\phi = \pi/4$ . In the linear response regime it grows linearly with  $\Delta\mu$  and it obeys an odd symmetry relation,  $\mu_P(\phi) = -\mu_P(-\phi)$ . Beyond linear response  $\mu_P$  does not follow neither an even nor an odd phase symmetry, but at large enough biases it is independent of the sign of the phase.

Fig. 6 displays results when spatial asymmetry in the form  $\gamma_L \neq \gamma_R$  is implemented. Here we observe that  $\Delta I \neq \mathcal{R}$ , and that the probe chemical potential does not satisfy an odd symmetry with the magnetic phase, even in the linear response regime.

As the breakdown of the MF symmetries (51) occurs under a spatial asymmetry in the presence of inelastic effects, we study next the role of  $\gamma_P$ ,  $\Delta\gamma \equiv \gamma_R - \gamma_L$  and the metals temperature  $\beta_a^{-1}$  on these relations.

In Fig. 7 (a)-(b) we extract  $\mathcal{D}$ , and present it along with  $\mathcal{R}$  as a function of  $\Delta\gamma$ . We note that the symmetry of  $\mathcal{R}$  is feasibly broken with small spatial asymmetry, while  $\mathcal{D}$  is more robust. The role of the coupling strength  $\gamma_P$  is considered in Fig. 8. First, in spatially symmetric systems we confirm again that the MF relations (51) are satisfied, and we note that as  $\gamma_P$  increases, the variation of  $\mathcal{D}$  and  $\mathcal{R}$  with phase is fading out. Quite interestingly, the rectification contribution  $\mathcal{R}$  may flip sign with  $\gamma_P$ , for a range of phases. (The sign of  $\mathcal{R}$  reflects whether the total current has a larger magnitude in the forward or backward bias polarity). Second, when a spatial asymmetry is introduced we note a strong breakdown of the MF phase symmetry for  $\mathcal{R}$ , while the coefficient  $\mathcal{D}$  still closely follows the MF symmetry<sup>33</sup>. Interestingly, with

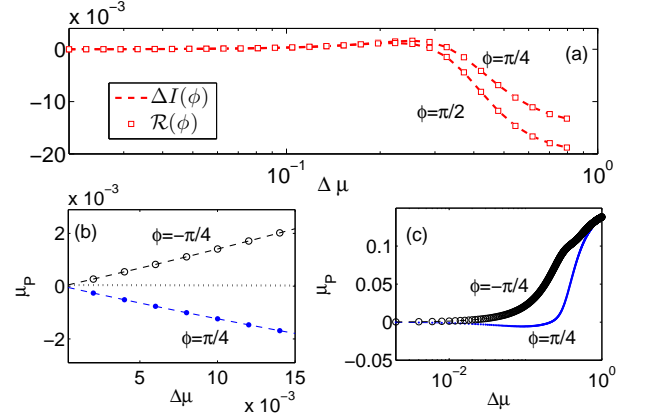


FIG. 5: (a) MF symmetry and rectification in spatially symmetric junctions. (b) Probe chemical potential in the linear response regime. (c) Probe chemical potential beyond linear response. The junction's parameters are  $\epsilon_1 = \epsilon_2 = 0.15$ ,  $\gamma_P = 0.1$ ,  $\beta_a = 50$  and  $\gamma_L = \gamma_R = 0.05$ .

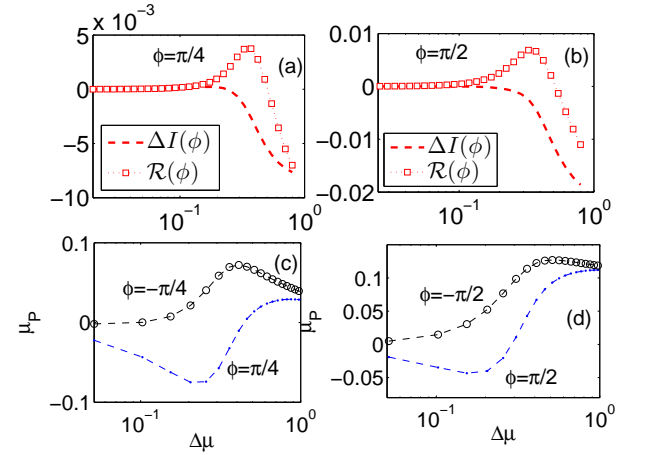


FIG. 6: Breakdown of the MF symmetry relations for spatially asymmetric junctions,  $\gamma_L = 0.05 \neq \gamma_R = 0.2$ . (a)-(b)  $\Delta I$  (dashed) and  $\mathcal{R}$  (square) for  $\phi = \pi/4$  and  $\pi/2$ . The corresponding probe potential is displayed in panel (c) for  $\phi = \pm\pi/4$  and in panel (d) for  $\phi = \pm\pi/2$ . Other parameters are  $\epsilon_1 = \epsilon_2 = 0.15$ ,  $\gamma_P = 0.1$  and  $\beta_a = 50$ .

increasing  $\gamma_P$  the variation of  $\mathcal{D}$  with phase is washed out (panel d), but even conductance terms show a stronger alteration with  $\phi$  (panel c). Thus, even and odd conductance terms respond distinctively to decohering and inelastic processes.

In Fig. 9 we consider the role of the reservoirs temperatures on the conductance coefficients. With increasing temperature a monotonic erosion of the amplitude of all conductance terms with phase takes place. This should be contrasted to the non-monotonic role of  $\gamma_P$  on  $\mathcal{R}$ , as exposed in Fig. 7.

Inspecting e.g., Fig. 9 we point out that in our construction  $\mathcal{R}(\phi = 0) = 0$ , even in the presence of geometrical asymmetry, see discussion following Eq. (46).

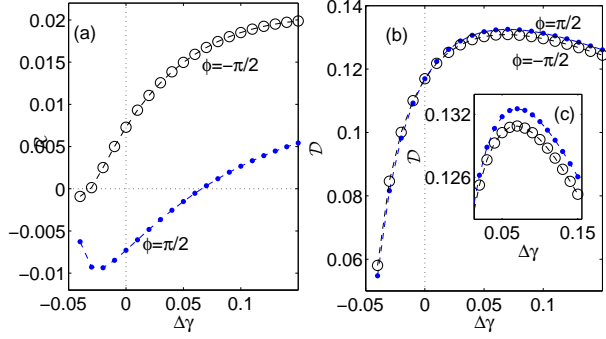


FIG. 7: (a)-(b) Even  $\mathcal{R}$  and odd  $\mathcal{D}$  conductance coefficients as a function of the coupling asymmetry  $\Delta\gamma = \gamma_R - \gamma_L$  with  $\gamma_L = 0.05$ . (c) Zoom over  $\mathcal{D}$ . Other parameters are  $\epsilon_1 = \epsilon_2 = 0.15$ ,  $\gamma_P = 0.1$ ,  $\Delta\mu = 0.4$  and  $\beta_a = 50$ .

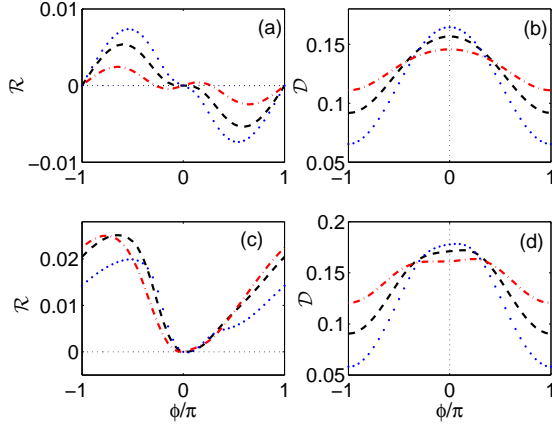


FIG. 8: Effect of the voltage probe coupling energy on even ( $\mathcal{R}$ ) and odd ( $\mathcal{D}$ ) conductance terms. (a)-(b) Spatially symmetric system,  $\gamma_L = \gamma_R = 0.05$ . (c)-(d) Spatially asymmetric junction,  $\gamma_L = 0.05 \neq \gamma_R = 0.2$ .  $\gamma_P = 0.1$  (dot),  $\gamma_P = 0.2$  (dashed line) and  $\gamma_P = 0.4$  (dashed-dotted). Light dotted lines represent symmetry lines. Other parameters are  $\Delta\mu = 0.4$ ,  $\epsilon_1 = \epsilon_2 = 0.15$ ,  $\beta_a = 50$ .

We recall that many-body effects are presented here effectively, thus this observation is not trivial given the common expectation that the combination of many-body interactions and spatial asymmetry should bring in the current rectification effect<sup>55</sup>. Indeed, extended models in which the system is connected to the reservoirs indirectly, through “linker” states, present rectification even at zero magnetic field, as long as both spatial asymmetry and inelastic effects are introduced<sup>13</sup>.

The scan of the current with  $\epsilon_d = \epsilon_{1,2}$  is presented in Fig. 10. When  $\epsilon_d > \Delta\mu$ , Onsager symmetry is practically respected since the linear response limit is practiced, providing  $\Delta I \sim \mathcal{R} \sim 0$ . More significantly, this figure reveals the MFGV symmetry (64), valid irrespective of spatial asymmetries and many-body (inelastic) effects. This symmetry immediately implies that at the

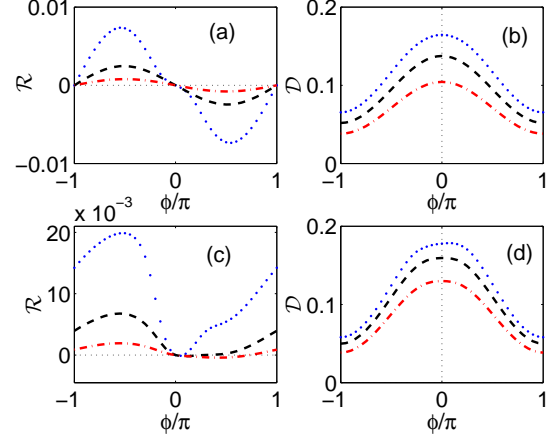


FIG. 9: Temperature dependence of even and odd conductance terms. (a)-(b) Spatially symmetric system,  $\gamma_L = \gamma_R = 0.05$ . (c)-(d) Spatially asymmetric system,  $\gamma_L = 0.05 \neq \gamma_R = 0.2$ . In all panels  $\beta_a = 50$  (dots),  $\beta_a = 10$  (dashed line) and  $\beta_a = 5$  (dashed-dotted line). The light dotted lines mark symmetry lines. Other parameters are  $\Delta\mu = 0.4$ ,  $\gamma_P = 0.1$  and  $\epsilon_1 = \epsilon_2 = 0.15$ .

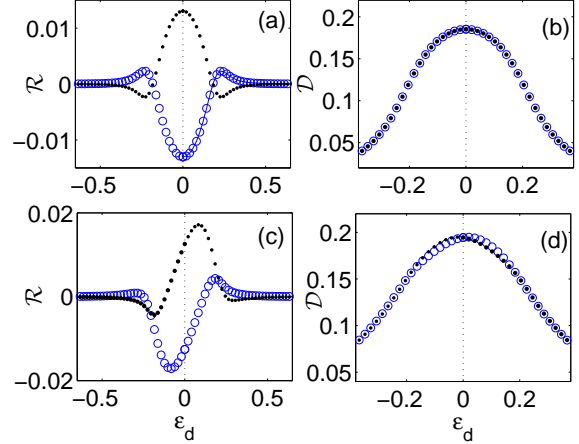


FIG. 10: Magnetic field- gate voltage (MFGV) symmetries. (a)-(b) Even and odd conductance terms for a spatially symmetric junction with  $\gamma_L = \gamma_R = 0.05$ . (c)-(d) Even and odd conductance terms for  $\gamma_L = 0.05$ ,  $\gamma_R = 0.2$ , demonstrating  $\mathcal{R}(\epsilon_d, \phi) = -\mathcal{R}(-\epsilon_d, -\phi)$ ,  $\mathcal{D}(\epsilon_d, \phi) = \mathcal{D}(-\epsilon_d, -\phi)$ . In all cases  $\phi = -\pi/4$  (small dots) and  $\phi = \pi/4$  (empty circle),  $\Delta\mu = 0.4$ ,  $\gamma_P = 0.1$  and  $\beta_a = 50$ .

so-called “symmetric point”, when  $\epsilon_d = 0$  (set at the Fermi energy),  $\mathcal{R}(\phi)$  is an odd function of the magnetic flux irrespective of spatial asymmetries. This behavior is displayed in Fig. 11. Also note that at the symmetric point the probe chemical potential does not manifest a linear response limit: It is identically zero for symmetric setups, and it satisfies  $\mu_P(\phi) = \mu_P(-\phi)$  far from equilibrium for setups with a broken inversion symmetry, see Fig. 12.

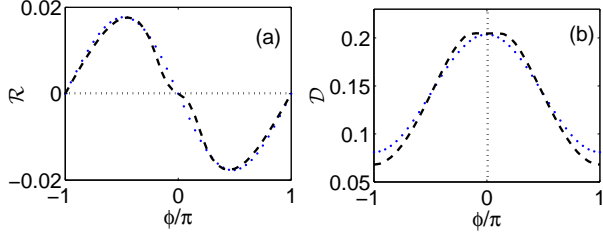


FIG. 11: MF symmetries at the symmetric point  $\epsilon_d = \epsilon_1 = \epsilon_2 = 0$ . (a) Even  $\mathcal{R}$  (b) odd  $\mathcal{D}$  conductance terms for spatially symmetric  $\gamma_L = \gamma_R = 0.05$  (dots) and asymmetric situations  $\gamma_L = 0.05$ ,  $\gamma_R = 0.2$  (dashed lines). Other parameters are  $\Delta\mu = 0.4$ ,  $\gamma_P = 0.1$  and  $\beta_a = 50$ .

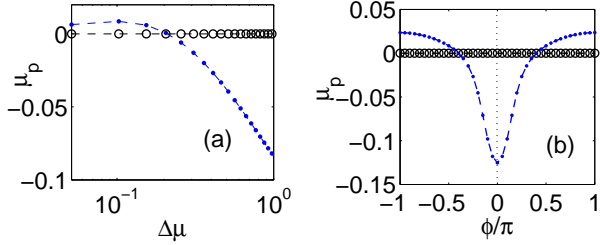


FIG. 12: (a)-(b) Probe chemical potential at the symmetric point for spatially symmetric  $\gamma_L = \gamma_R = 0.05$  (circles), and asymmetric  $\gamma_L = 0.05 \neq \gamma_R = 0.2$  cases (dots). The lines contain the overlapping  $\phi = \pm\pi/4$  results. Other parameters are  $\Delta\mu = 0.4$ ,  $\beta_a = 50$  and  $\gamma_P = 0.1$ .

### C. Nonlinear transport with non-dissipative inelastic effects

The simulations presented throughout Figs. 5-12 were obtained under the voltage probe condition, thus heat dissipation takes place at the probe. In Fig. 13 we show that the breakup of the MF symmetries occurs in spatially asymmetric setups under the more restrictive voltage-temperature probe, when only *non-dissipative* inelastic effects are allowed. We again note that the breakdown of the phase symmetry of  $\mathcal{D}$  is small, one order of magnitude below the variation in  $\mathcal{R}$ .

## VIII. SUMMARY

We have studied the role of elastic and inelastic scattering effects on magnetic field symmetries of nonlinear conductance terms using Büttiker's probe technique. For spatially symmetric junctions we proved the validity of the MF symmetries  $\mathcal{D}(\phi) = \mathcal{D}(-\phi)$  and  $\mathcal{R}(\phi) = -\mathcal{R}(-\phi)$ , though many-body inelastic effects, introduced via the probe, are asymmetric in magnetic flux. We

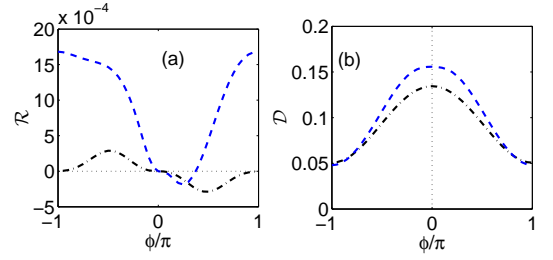


FIG. 13: Voltage-temperature probe. (a)  $\mathcal{R}$  and (b)  $\mathcal{D}$  in spatially symmetric case (dashed-dotted lines)  $\gamma_{L,R} = 0.05$  and asymmetric setups (dashed lines)  $\gamma_L = 0.05 \neq \gamma_R = 0.2$ .  $\beta_a = 10$ ,  $\gamma_P = 0.1$ ,  $\epsilon_{1,2} = 0.15$ .

demonstrated the breakdown of these MF symmetries when the junction has a left-right asymmetry, in the presence of inelastic effects. Using a double-dot AB interferometer model we showed that it respects more general MFGV symmetry relations,  $\mathcal{R}(\epsilon_d, \phi) = -\mathcal{R}(-\epsilon_d, -\phi)$  and  $\mathcal{D}(\epsilon_d, \phi) = \mathcal{D}(-\epsilon_d, -\phi)$ .

The rectification effect, of fundamental and practical interest, is realized by combining many-body interactions with a broken symmetry: broken spatial inversion symmetry or a broken time reversal symmetry. Rectifiers of the first type have been extensively investigated theoretically and experimentally, including electronic rectifiers, thermal rectifiers<sup>55</sup> and acoustic rectifiers<sup>56</sup>. In parallel, optical and spin rectifiers were designed based on a broken time reversal symmetry, recently realized e.g. by engineering parity-time meta-materials<sup>57</sup>.

The model system investigated in Secs.VI-VII, the double-dot AB junction, offers a feasible setup for devising broken-time reversal rectifiers: We found that  $\mathcal{R} \neq 0$  when two conditions are simultaneously met: the magnetic flux obeys  $\phi \neq 2\pi n$ ,  $n$  is an integer, and the probe introduces inelastic effects. However, when time-reversal symmetry is maintained (when the flux obeys  $\phi = 2n\pi$ ) our model does not provide the rectification effect even if the spatial mirror symmetry is broken. The technical reason is that in our minimal construction both dots are coupled to the  $L$  and  $R$  metals directly, with an energy independent hybridization constant. In extended models when the ring is coupled indirectly to the  $L$  and  $R$  metals, through a spacer state, geometrical rectification may develop even in the absence of a magnetic flux.

It is of interest to verify the results of this work by adopting a microscopic model with genuine many-body interactions<sup>58-60</sup>, by modeling a quantum point contact<sup>61,62</sup> or an equilibrated phonon bath, exchanging energy with the junction's electronic degrees of freedom. This could be done by extending numerical and analytic studies, e.g., Refs.<sup>63-65</sup>, to the nonlinear regime. It is also of interest to obtain the MF and the MFGV symmetries using a full-counting statistics approach<sup>25,66</sup>.

Future studies will be devoted to the analysis of the thermoelectric effect under broken time-reversal symmetry<sup>8-10,65,67-69</sup> in the far-from-equilibrium regime,

and to the study of quantum transport, far-from-equilibrium, in networks with broken time-reversal symmetry<sup>70</sup>.

### Acknowledgments

DS acknowledges support from the Natural Science and Engineering Research Council of Canada. The work of SB has been supported by the Early Research Award of DS. The authors acknowledge R. Härtle for useful comments.

### Appendix A: Charge conjugation symmetries for a double-dot AB interferometer

We derive the MFGV symmetry relations by considering a double-dot interferometer model which does not

necessarily acquire a spatial symmetry. Given the Hamiltonian (52)-(55), we introduce a charge conjugation operator  $\mathcal{C}$  that acts to replace an electron by a hole<sup>71</sup>,

$$\begin{aligned}\mathcal{C}(\epsilon_d) &= -\epsilon_d, & \mathcal{C}(\epsilon_k) &= -\epsilon_k, \\ \mathcal{C}(v_{n,j}e^{i\phi_n}) &= -v_{n,j}^*e^{-i\phi_n}, & \mathcal{C}(\langle a^\dagger a \rangle) &= 1 - \langle a^\dagger a \rangle.\end{aligned}\tag{A1}$$

Here  $a^\dagger$  and  $a$  are fermionic creation and annihilation operators, respectively. First, we need to find what symmetries does the probe chemical potential obey. We achieve this by studying the probe condition (44) as is, under reversed bias voltage, and under charge conjugation. Note that in our model the transmission function satisfies  $\mathcal{T}(\epsilon, \epsilon_d, \phi) = \mathcal{T}(-\epsilon, -\epsilon_d, -\phi)$ , i.e. it is invariant under charge conjugation. The probe condition fulfills

---


$$\int d\epsilon(\mathcal{T}_{P,L} + \mathcal{T}_{P,R})f_P(\mu_P(\epsilon_d, \phi, \mu_L, \mu_R)) = \int d\epsilon(\mathcal{T}_{L,P}f_L + \mathcal{T}_{R,P}f_R)\tag{A2}$$

$$\int d\epsilon(\mathcal{T}_{P,L} + \mathcal{T}_{P,R})f_P(\mu_P(\epsilon_d, \phi, \mu_R, \mu_L)) = \int d\epsilon(\mathcal{T}_{L,P}f_R + \mathcal{T}_{R,P}f_L).\tag{A3}$$

$$\int d\epsilon(\mathcal{T}_{P,L} + \mathcal{T}_{P,R})[1 - f_P(-\mu_P(-\epsilon_d, -\phi, \mu_L, \mu_R))] = \int d\epsilon(\mathcal{T}_{L,P}[1 - f_R] + \mathcal{T}_{R,P}[1 - f_L])\tag{A4}$$


---

For clarity, we explicitly noted the dependence of  $f_P$  on the chemical potential  $\mu_P$ , itself obtained given the set of parameters  $\epsilon_d$ ,  $\phi$ , and  $\mu_{L,R}$ . The last relation [Eq. (A4)] has been derived by noting that

$$\begin{aligned}f_\nu(-\epsilon, \mu_\nu) &= [e^{\beta(-\epsilon - \mu_\nu)} + 1]^{-1} \\ &= 1 - f_\nu(\epsilon, -\mu_\nu).\end{aligned}\tag{A5}$$

Since we use the convention  $\mu_L = -\mu_R$ , we conclude that  $f_L(-\epsilon, \mu_L) = 1 - f_R(\epsilon, \mu_R)$ . Next we omit the direct reference to the energy  $\epsilon$  within  $\mathcal{T}$  and the Fermi functions. Also, we do not write the phase  $\phi$  in the transmission function, unless necessary to eliminate confusion. Equation (A4) now reduces to

$$\begin{aligned}&\int d\epsilon(\mathcal{T}_{P,L} + \mathcal{T}_{P,R})f_P(-\mu_P(-\epsilon_d, -\phi, \mu_L, \mu_R)) \\ &= \int d\epsilon(\mathcal{T}_{L,P}f_R + \mathcal{T}_{R,P}f_L).\end{aligned}\tag{A6}$$


---

Comparing this to Eq. (A3), we immediately note that

$$f_P(-\mu_P(-\epsilon_d, -\phi, \mu_L, \mu_R)) = f_P(\mu_P(\epsilon_d, \phi, \mu_R, \mu_L)).\tag{A7}$$

Since all reservoirs are maintained at  $T_a$  this implies that

$$\mu_P(\epsilon_d, \phi, \mu_L, \mu_R) = -\mu_P(-\epsilon_d, -\phi, \mu_R, \mu_L).\tag{A8}$$

This relation should be compared to Eq. (48), valid for spatially symmetric systems. We now utilize Eq. (A7) and derive the symmetry relations for  $\mathcal{R}$  and  $\mathcal{D}$ . We recall the explicit expressions for these measures, see definitions in Sec. III,

$$\begin{aligned}\mathcal{R} &= \frac{1}{2} \int d\epsilon \mathcal{T}_{P,L} [f_L + f_R - f_P(\mu_P(\epsilon_d, \phi, \mu_L, \mu_R)) - f_P(\mu_P(\epsilon_d, \phi, \mu_R, \mu_L))] \\ \mathcal{D} &= \frac{1}{2} \int d\epsilon \left\{ (\mathcal{T}_{L,R} + \mathcal{T}_{L,P} + \mathcal{T}_{R,L})(f_L - f_R) - \mathcal{T}_{P,L} [f_P(\mu_P(\epsilon_d, \phi, \mu_L, \mu_R)) - f_P(\mu_P(\epsilon_d, \phi, \mu_R, \mu_L))] \right\}\end{aligned}\tag{A9}$$

The charge-conjugated expressions satisfy

$$\begin{aligned}
\mathcal{C}(\mathcal{R}) &= \frac{1}{2} \int d\epsilon \mathcal{T}_{P,L} \{ [1 - f_R] + [1 - f_L] - [1 - f_P(-\mu_P(-\epsilon_d, -\phi, \mu_L, \mu_R))] - [1 - f_P(-\mu_P(-\epsilon_d, -\phi, \mu_R, \mu_L))] \} \\
&= -\frac{1}{2} \int d\epsilon \mathcal{T}_{P,L} \{ f_R + f_L - f_P(-\mu_P(-\epsilon_d, -\phi, \mu_L, \mu_R)) - f_P(-\mu_P(-\epsilon_d, -\phi, \mu_R, \mu_L)) \} \\
&= -\mathcal{R}
\end{aligned} \tag{A10}$$

The last equality is reached by using Eq. (A7). Similarly, we obtain the symmetry of odd conductance terms as

$$\begin{aligned}
\mathcal{C}(\mathcal{D}) &= \frac{1}{2} \int d\epsilon \left\{ (\mathcal{T}_{L,R} + \mathcal{T}_{L,P} + \mathcal{T}_{R,L})(1 - f_R - 1 + f_L) \right. \\
&\quad \left. - \mathcal{T}_{P,L} [1 - f_P(-\mu_P(-\epsilon_d, -\phi, \mu_L, \mu_R))] - 1 + f_P(-\mu_P(-\epsilon_d, -\phi, \mu_R, \mu_L)) \right\} \\
&= \frac{1}{2} \int d\epsilon \left\{ (\mathcal{T}_{L,R} + \mathcal{T}_{L,P} + \mathcal{T}_{R,L})(f_L - f_R) + \mathcal{T}_{P,L} [f_P(-\mu_P(-\epsilon_d, -\phi, \mu_L, \mu_R))] - f_P(-\mu_P(-\epsilon_d, -\phi, \mu_R, \mu_L)) \right\} \\
&= \mathcal{D}
\end{aligned} \tag{A11}$$

In the double-dot interferometer model these relations translate to the MFGV symmetries,

$$\begin{aligned}
\mathcal{R}(\epsilon_d, \phi) &= -\mathcal{R}(-\epsilon_d, -\phi), \\
\mathcal{D}(\epsilon_d, \phi) &= \mathcal{D}(-\epsilon_d, -\phi).
\end{aligned} \tag{A12}$$

For compactness, the derivation above has been performed assuming  $\epsilon_d = \epsilon_1 = \epsilon_2$ . It is trivial to note that our results are valid beyond degeneracy.

## Appendix B: MF symmetries of nonlinear heat transport

In this Appendix we study symmetry relations of the electronic heat current under nonzero magnetic flux and a temperature bias  $T_L \neq T_R$ , in the absence of a potential bias,  $\mu_a = \mu_L = \mu_R = \mu_P$ . Using the temperature probe (10), we demand that heat dissipation at the probe diminishes,  $Q_P = 0$ , but allow for charge dissipation. We now express the  $L$  to  $R$  heat current  $Q_{\Delta T} \equiv Q_L = -Q_R$  in powers of the temperature bias as

$$Q_{\Delta T}(\phi) = K_1(\phi)\Delta T + K_2(\phi)(\Delta T)^2 + K_3(\phi)(\Delta T)^3 + \dots, \tag{B1}$$

where  $K_{n>1}$  are the nonlinear conductance coefficients. These coefficients depend on the junction parameters: energy, hybridization and possibly the temperature  $T_a = (T_L + T_R)/2$ . We define next symmetry measures for the heat current  $Q_{\Delta T}$ , parallel to Eqs. (16)-(22). First, we

collect even conductance terms into  $\mathcal{R}_{\Delta T}$ ,

$$\begin{aligned}
\mathcal{R}_{\Delta T}(\phi) &\equiv \frac{1}{2}[Q(\phi) + \bar{Q}(\phi)] \\
&= K_2(\phi)(\Delta T)^2 + K_4(\phi)(\Delta T)^4 + \dots \\
&= \int \frac{\mathcal{T}_{P,L} - \mathcal{T}_{P,R}}{4} (f_L + f_R - f_P(\phi) - \bar{f}_P(\phi)) (\epsilon - \mu_a) d\epsilon
\end{aligned} \tag{B2}$$

Here  $\bar{Q}$  is defined as the heat current obtained upon interchanging the temperatures of the  $L$  and  $R$  terminals. We also study the behavior of odd conductance terms,

$$\mathcal{D}_{\Delta T}(\phi) \equiv K_1(\phi)\Delta T + K_3(\phi)(\Delta T)^3 + \dots \tag{B3}$$

In the absence of the probe and in the linear response limit the heat current satisfies an even phase symmetry,  $Q_{\Delta T}(\phi) = Q_{\Delta T}(-\phi)$ . Deviations from this symmetry are collected into the measure

$$\begin{aligned}
\Delta Q_{\Delta T} &= \frac{1}{2} [Q_{\Delta T}(\phi) - Q_{\Delta T}(-\phi)] \\
&= \frac{1}{2} \int [\mathcal{T}_{L,R} - \mathcal{T}_{R,L}] (\epsilon - \mu_a) f_R d\epsilon \\
&\quad + \frac{1}{2} \int [\mathcal{T}_{L,P} f_P(-\phi) - \mathcal{T}_{P,L} f_P(\phi)] (\epsilon - \mu_a) d\epsilon.
\end{aligned} \tag{B4}$$

*Linear response regime.* We repeat the derivation of Sec. IV, and find that in the linear response regime,  $T_L = T_a + \delta T_L$ ,  $T_R = T_a + \delta T_R$ , the probe temperature  $T_P = T_a + \delta T_P$  obeys

$$\delta T_P(\phi) = \frac{\int d\epsilon \left( \frac{-\partial f_a}{\partial \epsilon} \right) \frac{(\epsilon - \mu_a)^2}{T_a} (\delta T_L \mathcal{T}_{L,P} + \delta T_R \mathcal{T}_{R,P})}{\int d\epsilon \left( \frac{-\partial f_a}{\partial \epsilon} \right) \frac{(\epsilon - \mu_a)^2}{T_a} (\mathcal{T}_{P,L} + \mathcal{T}_{P,R})} \tag{B5}$$

Using this relation, one can readily repeat the steps in Sec. IV and prove that  $\mathcal{R}_{\Delta T} = 0$ , thus  $Q_{\Delta T}(\phi) = \mathcal{D}_{\Delta T}(\phi) = Q_{\Delta T}(-\phi)$ .

*Symmetry relations far-from-equilibrium.* We discuss here symmetry relations for spatially symmetric junctions. We adapt the temperature probe condition (10) to three situations. First, the standard expression is given by

$$\begin{aligned} & \int d\epsilon (\mathcal{T}_{P,L} + \mathcal{T}_{P,R}) f_P(\phi) (\epsilon - \mu_a) \\ &= \int d\epsilon (\mathcal{T}_{L,P} f_L + \mathcal{T}_{R,P} f_R) (\epsilon - \mu_a). \end{aligned} \quad (\text{B6})$$

We reverse the magnetic phase and get

$$\begin{aligned} & \int d\epsilon (\mathcal{T}_{L,P} + \mathcal{T}_{R,P}) f_P(-\phi) (\epsilon - \mu_a) \\ &= \int d\epsilon (\mathcal{T}_{P,L} f_L + \mathcal{T}_{P,R} f_R) (\epsilon - \mu_a). \end{aligned} \quad (\text{B7})$$

Similarly, when interchanging the temperatures  $T_L$  and  $T_R$  we look for the probe distribution  $f_P$  which satisfies

$$\begin{aligned} & \int d\epsilon (\mathcal{T}_{P,L} + \mathcal{T}_{P,R}) \bar{f}_P(\phi) (\epsilon - \mu_a) \\ &= \int d\epsilon (\mathcal{T}_{L,P} f_R + \mathcal{T}_{R,P} f_L) (\epsilon - \mu_a). \end{aligned} \quad (\text{B8})$$

Note that  $f_P(\phi)$ ,  $f_P(-\phi)$  and  $\bar{f}_P(\phi)$  are required to follow a Fermi-Dirac form. The temperature  $\beta_P$  should be obtained so as to satisfy the probe condition. If the junction is left-right symmetric, the mirror symmetry  $\mathcal{T}_{P,L}(\phi) = \mathcal{T}_{R,P}(\phi)$  applies. We use this relation in Eqs. (B7) and (B8) and conclude that the probe distribution obeys

$$\bar{f}_P(\phi) = f_P(-\phi). \quad (\text{B9})$$

This directly implies that  $(\mu_a = \mu_L = \mu_R = \mu_P)$

$$\bar{\beta}_P(\phi) = \beta_P(-\phi). \quad (\text{B10})$$

Note that  $\beta_P(\phi)$  does not need to obey any particular magnetic phase symmetry. The deviation from phase rigidity, Eq. (B4), can be expressed using the heat current flowing into the  $R$  terminal,

$$\begin{aligned} \Delta Q_{\Delta T} &= \frac{1}{2} \int (\epsilon - \mu_a) [(\mathcal{T}_{L,R} - \mathcal{T}_{R,L}) f_L \\ &\quad - \mathcal{T}_{R,P} f_P(-\phi) + \mathcal{T}_{P,R} f_P(\phi)] d\epsilon. \end{aligned} \quad (\text{B11})$$

We define  $\Delta Q_{\Delta T}$  as the average of Eqs. (B4) and (B11),

$$\begin{aligned} \Delta Q_{\Delta T} &= \frac{1}{4} \int d\epsilon (\epsilon - \mu_a) \left[ (\mathcal{T}_{L,R} - \mathcal{T}_{R,L}) (f_L + f_R) \right. \\ &\quad \left. + (\mathcal{T}_{L,P} - \mathcal{T}_{R,P}) f_P(-\phi) + (\mathcal{T}_{P,R} - \mathcal{T}_{P,L}) f_P(\phi) \right]. \end{aligned}$$

Using the identities  $\mathcal{T}_{L,R} - \mathcal{T}_{R,L} = \mathcal{T}_{P,L} - \mathcal{T}_{L,P}$  and  $\mathcal{T}_{P,L} = \mathcal{T}_{R,P}$ , the latter is valid in geometrically symmetric junctions, we get

$$\begin{aligned} & \Delta Q_{\Delta T}(\phi) \\ &= \frac{1}{4} \int (\mathcal{T}_{P,L} - \mathcal{T}_{P,R}) (f_L + f_R - f_P(\phi) - \bar{f}_P(\phi)) (\epsilon - \mu_a) d\epsilon \\ &= \mathcal{R}_{\Delta T}(\phi) = -\mathcal{R}_{\Delta T}(-\phi). \end{aligned} \quad (\text{B12})$$

This concludes our derivation that under a temperature bias even (odd) heat conductance coefficients satisfy an odd (even) magnetic field symmetry,

$$\begin{aligned} \mathcal{R}_{\Delta T}(\phi) &= -\mathcal{R}_{\Delta T}(-\phi) = \Delta Q_{\Delta T}(\phi), \\ \mathcal{D}_{\Delta T}(\phi) &= \mathcal{D}_{\Delta T}(-\phi), \end{aligned} \quad (\text{B13})$$

as long as the junction acquires a spatial mirror symmetry.

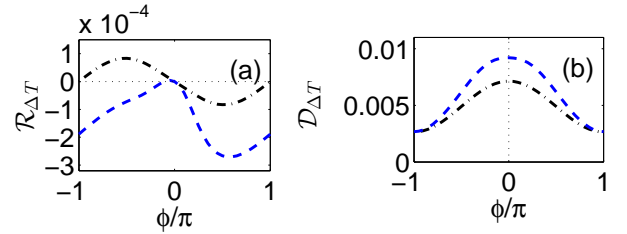


FIG. 14: Magnetic field symmetries of (a) even and (b) odd electronic heat conductance terms. Spatially symmetric system (dashed dotted),  $\gamma_L = \gamma_R = 0.05$ . Spatially asymmetric junction (dashed),  $\gamma_L = 0.05 \neq \gamma_R = 0.2$ . Light dotted lines represent the symmetry lines. Other parameters are  $T_L = 0.15$ ,  $T_R = 0.05$ ,  $\epsilon_1 = \epsilon_2 = 0.15$ ,  $\gamma_P = 0.1$ ,  $\mu_a = \mu_L = \mu_R = \mu_P = 0$ .

We adopt the double-dot model (52) presented in Sec. VI and study its heat current behavior. In the absence of the probe, assuming for simplicity degeneracy and spatial symmetry,  $\gamma/2 = \gamma_{L,R}$ , we obtain

$$Q_L(\phi) = \int d\epsilon (\epsilon - \mu_a) \frac{\gamma^2 (\epsilon - \epsilon_d)^2 \cos^2 \frac{\phi}{2}}{\left[ (\epsilon - \epsilon_d)^2 - \frac{\gamma^2}{4} \sin^2 \frac{\phi}{2} \right]^2 + \gamma^2 (\epsilon - \epsilon_d)^2} [f_L(\epsilon) - f_R(\epsilon)],$$

satisfying the Onsager symmetry. Fig. 14 displays the MF symmetries, and their violation, Deviations from

phase symmetry for  $\mathcal{D}_{\Delta T}$  are small, of the order of  $10^{-5}$ .

- 
- <sup>1</sup> S. Andergassen, V. Meden, H. Schoeller, J. Splettstoesser, and M. R. Wegewijs, *Nanotechnology* **21**, 272001 (2010), and references therein.
- <sup>2</sup> N. G. van Kampen, *Stochastic processes in physics and chemistry*, (North Holland, 1981).
- <sup>3</sup> H.-P. Breuer and F. Petruccione, *The Theory of Open Quantum Systems* (Oxford University Press, Oxford, UK, 2002).
- <sup>4</sup> M. Büttiker, *Phys. Rev. B* **32**, 1846 (1985); *Phys. Rev. B* **33**, 3020 (1986), *IBM J. Res. Dev.* **32**, 63 (1988).
- <sup>5</sup> J. L. D'amato and H. M. Pastawski, *Phys. Rev. B* **41**, 7411 (1990).
- <sup>6</sup> T. Ando, *Surf. Sci.* **361-362**, 270 (1996).
- <sup>7</sup> P. A. Jacquet, *J. Stat. Phys.* **134**, 709 (2009).
- <sup>8</sup> K. Saito, G. Benenti, G. Casati, and T. Prosen, *Phys. Rev. B* **84**, 201306 (2011).
- <sup>9</sup> V. Balachandran, G. Benenti, and G. Casati, *Phys. Rev. B* **87**, 165419 (2013).
- <sup>10</sup> K. Brandner, K. Saito, and U. Seifert, *Phys. Rev. Lett.* **110**, 070603 (2013).
- <sup>11</sup> J. P. Bergfield, S. M. Story, R. C. Stafford, and C. A. Stafford, *ACS Nano* **7**, 4429 (2013).
- <sup>12</sup> Y. Ming, Z. Wang, Z. Ding, H. Li, *New J. Phys.* **12**, 103041 (2010).
- <sup>13</sup> M. Bandyopadhyay and D. Segal, *Phys. Rev. E* **84**, 011151 (2011).
- <sup>14</sup> Ph. A. Jacquet and C.-A. Pillet, *Phys. Rev. B* **85**, 125120 (2012).
- <sup>15</sup> K. Saaskilahti, J. Oksanen, and J. Tulkki, *Phys. Rev. E* **88**, 012128 (2013).
- <sup>16</sup> P. Rouleau, F. Portier, P. Roche, A. Cavanna, G. Faini, U. Gennser, and D. Mailly, *Phys. Rev. Lett.* **102**, 236802 (2009).
- <sup>17</sup> M. J. M. de Jong and C. W. J. Beenakker, *Physica A* **230**, 219 (1996).
- <sup>18</sup> S. A. van Langen and M. Büttiker, *Phys. Rev. B* **56**, R1680 (1997).
- <sup>19</sup> H.-L. Engquist and P. W. Anderson, *Phys. Rev. B* **24**, 1151 (1981).
- <sup>20</sup> D. Roy and A. Dhar, *Phys. Rev. B* **75**, 195110 (2007).
- <sup>21</sup> F. Bonetto, J. Lebowitz, and L. Rey-Bellet, *Mathematical Physics 2000* (World Scientific, Singapore, 2000), pp. 128150.
- <sup>22</sup> A. Dhar and D. Roy, *J. Stat. Phys.* **125**, 801 (2006).
- <sup>23</sup> D. Roy, *Phys. Rev. E* **77**, 062102 (2008).
- <sup>24</sup> D. Segal, *Phys. Rev. E* **79**, 012103 (2009).
- <sup>25</sup> S. Pilgram, P. Samuelsson, H. Förster, and M. Büttiker, *Phys. Rev. Lett.* **97**, 066801 (2006).
- <sup>26</sup> L. Onsager, *Phys. Rev.* **37**, 405 (1931); **38**, 2265 (1931); H. B. G. Casimir, *Rev. Mod. Phys.* **17**, 343 (1945).
- <sup>27</sup> Y. Imry, *Introduction to Mesoscopic Physics*, 2nd ed. (Oxford University Press, Oxford, 2002).
- <sup>28</sup> A. Yacoby, M. Heiblum, D. Mahalu, and H. Shtrikman, *Phys. Rev. Lett.* **74**, 4047 (1995).
- <sup>29</sup> A. Löfgren, C. A. Marlow, I. Shorubalko, R. P. Taylor, P. Omling, L. Samuelson, and H. Linke, *Phys. Rev. Lett.* **92**, 046803 (2004).
- <sup>30</sup> C. A. Marlow, R. P. Taylor, M. Fairbanks, I. Shorubalko, and H. Linke, *Phys. Rev. Lett.* **96**, 116801 (2006).
- <sup>31</sup> H. Linke, W. D. Sheng, A. Svensson, A. Löfgren, L. Christensson, H. Q. Xu, P. Omling and P. E. Lindelof, *Phys. Rev. B* **61**, 15914 (2000).
- <sup>32</sup> J. Wei, M. Shimogawa, Z. Wang, I. Radu, R. Dormaier, and D. H. Cobden, *Phys. Rev. Lett.* **95**, 256601 (2005).
- <sup>33</sup> R. Leturcq, D. Sanchez, G. Götz, T. Ihn, K. Ensslin, D. C. Driscoll, and A. C. Gossard, *Phys. Rev. Lett.* **96**, 126801 (2006); R. Leturcq, R. Bianchetti, G. Götz, T. Ihn, K. Ensslin, D.C. Driscoll, and A. C. Gossard, *Physica E* **35**, 327 (2006).
- <sup>34</sup> L. Angers, E. Zakka-Bajjani, R. Deblock, S. Gueron, H. Bouchiat, A. Cavanna, U. Gennser, and M. Polianski, *Phys. Rev. B* **75**, 115309 (2007).
- <sup>35</sup> M. Sigrist, T. Ihn, K. Ensslin, M. Reinwald, and W. Wegscheider, *Phys. Rev. Lett.* **98**, 036805 (2007); T. Ihn, M. Sigrist, K. Ensslin, W. Wegscheider, and M. Reinwald, *New J. Phys.* **9**, 111 (2007).
- <sup>36</sup> G. M. Gusev, Z. D. Kvon, E. B. Olshanetsky, and A. Y. Plotnikov, *Europhys. Lett.* **88**, 47007 (2009).
- <sup>37</sup> F. G. G. Hernandez, G. M. Gusev, Z. D. Kvon, J. C. Portal, *Phys. Rev. B* **84**, 075332 (2011).
- <sup>38</sup> D. Sanchez and M. Büttiker, *Phys. Rev. Lett.* **93**, 106802 (2004); *Int. J. Quantum Chem.* **105**, 906 (2005).
- <sup>39</sup> B. Spivak and A. Zyuzin, *Phys. Rev. Lett.* **93**, 226801 (2004).
- <sup>40</sup> A. R. Hernandez and C. H. Lewenkopf, *Phys. Rev. Lett.* **103**, 166801 (2009).
- <sup>41</sup> T. Kubo, Y. Ichigo, and Y. Tokura, *Phys. Rev. B* **83**, 235310 (2011).
- <sup>42</sup> V. Puller, Y. Meir, M. Sigrist, K. Ensslin, and T. Ihn, *Phys. Rev. B* **80**, 035416 (2009).
- <sup>43</sup> S. Bedkihal, M. Bandyopadhyay, and D. Segal, arXiv:1306.6491
- <sup>44</sup> R. Landauer, *IBM J. Res. Dev.* **1**, 223 (1957).
- <sup>45</sup> M. Büttiker, *Phys. Rev. Lett.* **57**, 1761 (1986).
- <sup>46</sup> S. Datta, *Electric transport in Mesoscopic Systems* (Cambridge: Cambridge University Press 1995).
- <sup>47</sup> W. H. Press, B. P. Flannery, S. A. Teukosky, and W. T. Vetterling, *Numerical Recipes in C: The Art of Scientific Computing*, (Cambridge University Press 1992).
- <sup>48</sup> Persistent currents exist in at thermal equilibrium due to the absence of time-reversal symmetry. In our work here we consider only net charge transport. However, since persistent currents are antisymmetric in the magnetic field, we could add them to the definition of  $\mathcal{R}(\phi)$ , and our observations would be still valid.
- <sup>49</sup> Y. Meir and N. S. Wingreen, *Phys. Rev. Lett.* **68**, 2512 (1992).
- <sup>50</sup> J. Fransson, *Non-equilibrium nano-physics, a many body approach* Lecture Notes in Physics **809**, Springer (2010).
- <sup>51</sup> S. Bedkihal and D. Segal, *Phys. Rev. B* **85**, 155324 (2012).
- <sup>52</sup> M. W.-Y. Tu, W.-M. Zhang, J. Jin, O. Entin-Wohlman, and A. Aharony, *Phys. Rev. B* **86**, 115453 (2012).
- <sup>53</sup> S. Bedkihal, M. Bandyopadhyay, and D. Segal, *Phys. Rev. B* **87**, 045418 (2013).

- <sup>54</sup> B. Kubala and J. König, Phys. Rev. B **65**, 245301 (2002).
- <sup>55</sup> M. Terraneo, M. Peyrard, G. Casati, Phys. Rev. Lett. **88**, 094302 (2002); D. Segal, A. Nitzan, *ibid.* **94**, 034301 (2005); C. W. Chang et al., Science **314**, 1121 (2006).
- <sup>56</sup> X.-F. Li, X. Ni, L. Feng, M.-H. Lu, C. He, and Y.-F. Chen, Phys. Rev. Lett. **106**, 084301 (2011).
- <sup>57</sup> L. Feng, Y.-L. Xu, W. S. Fegadolli, M.-H. Lu, J. E. B. Oliveira, V. R. Almeida, Y.-F. Chen, and A. Scherer, Nature Materials **12**, 108 (2013).
- <sup>58</sup> E. Deyo, B. Spivak, and A. Zyuzin, Phys. Rev. B **74**, 104205 (2006).
- <sup>59</sup> A. Ueda and M. Eto, Phys. Rev. B **73**, 235353 (2006); New J. Phys. **9**, 119 (2007).
- <sup>60</sup> T. Kubo, Y. Tokura, and S. Tarucha, J. Phys. A: Math. Theor. **43**, 354020 (2010).
- <sup>61</sup> D. Sanchez and K. Kang, Phys. Rev. Lett. **100**, 036806 (2008).
- <sup>62</sup> V. I. Puller and Y. Meir, Phys. Rev. Lett. **104**, 256801 (2010).
- <sup>63</sup> O. Hod, R. Baer, and E. Rabani, Phys. Rev. Lett. **97**, 266803 (2006).
- <sup>64</sup> O. Hod, R. Baer, and E. Rabani, J. Phys. Condens. Matter **20**, 383201 (2008).
- <sup>65</sup> O. Entin-Wohlman and A. Aharony, Phys. Rev. B **85**, 085401 (2012).
- <sup>66</sup> K. Saito and Y. Utsumi, Phys. Rev. B **78**, 115429 (2008).
- <sup>67</sup> D. Sanchez and R. Lopez, Phys. Rev. Lett. **110**, 026804 (2013).
- <sup>68</sup> D. Sanchez and L. Serra, Phys. Rev. B **84**, 201307(R) (2011).
- <sup>69</sup> R. S. Whitney, Phys. Rev. B **87**, 115404 (2013).
- <sup>70</sup> Z. Zimboras, M. Faccin, Z. Kadar, J. D. Whitefield, B. P. Lanyon, and J. Biamonte, Scientific Reports **3:2361**, 1 (2013).
- <sup>71</sup> V. Kashcheyevs, A. Aharony, and O. Entin-Wohlman, Phys. Rev. B **73**, 125338 (2006).